ESTIMATING ZONAL FLOW CONTRIBUTIONS IN DEEP WATER ASSETS USING TEMPERATURE AND PRESSURE DATA

A Thesis

by

RAYHANA NAYEMA SOHEL

Submitted to the Office of Graduate and Professional Studies of
Texas A&M University
in partial fulfillment of the requirements for the degree of

MASTER OF SCIENCE

Chair of Committee,	A. Rashid Hasan
Committee Members,	Hadi Nasrabadi
	M.M. Faruque Hasan
Head of Department,	A. Daniel Hill

May 2017

Major Subject: Petroleum Engineering

ABSTRACT

Producing hydrocarbon from deep water assets is extremely challenging and expensive. A good estimate of rates from multiple pay zones is essential for well monitoring, surveillance, and workover decisions. Such information can be gleaned from flowing fluid pressure and temperature; deep-water wells are often well instrumented that offers such data on a continuous basis. In this study, we present a model that estimates zonal flow contributions based on energy and momentum balances. Kinetic and heat energy coming from the reservoir fluid to the production tubing is accounted for in the model. The momentum balance takes into account differing flow profile in both laminar and turbulent flows.

In addition, we used a recently developed analytical expression to calculate the effect of Joule-Thompson expansion on sandface fluid temperature to obtain an accurate estimate of the sandface temperature from reservoir temperature. The model developed can be applied to any reservoir with multiple pay zones and is especially useful for deep-water assets where production logging is practically impossible. We used available field data for multiphase flow to validate the model. Additionally, we verified the model using data generated by the model with randomly added inaccuracy to estimate rates and error bounds. Finally, we performed a sensitivity analysis on the various parameters in the model for a better understanding of the model.

ACKNOWLEDGEMENTS

First and foremost I would like to thank my advisor, Dr. A. Rashid Hasan for his continuous support and guidance throughout my years in Texas A&M University. I am grateful to him for all his time, patience and for the countless times he let me pick his brain. His enthusiasm and passion for his work has been truly inspirational.

I would also like to thank my committee members, Dr. Hadi Nasrabadi and Dr. M.M. Faruq Hasan for serving as my committee members. I appreciate their support for my work.

Thanks to my friends in here in College Station who has made me feel like family and has opened their homes to me.

Las but not least, I am grateful to my parents and my sister for supporting me in every academic decision I have made and for always believing in me.

CONTRIBUTORS AND FUNDING SOURCES

Contributors

Part 1, faculty committee recognition

This work was supervised by a thesis committee consisting of Dr. A. Rashid Hasan (advisor), Dr. Hadi Nasrabadi of the Department of Petroleum Engineering and Dr. M.M. Faruq Hasan of the Department of Chemical Engineering at Texas A&M University.

Part 2, student/collaborator contributions

All work for the thesis was completed independently by the student.

Funding Sources

There are no outside funding contributions to acknowledge related to the research and compilation of this document.

NOMENCLATURE

B_o	oil formation volume factor, bbl/STB
c_p	specific heat capacity, Btu/lb_m-^{0}F
C_J	Joule Thompson Coefficient, ft^3-^{0}F/Btu
d	tubing internal diameter, ft
f	friction factor
g_c	gravitational constant, 32.2 lb_m-ft/lb_f-s^2
h	formation thickness
h_c	heat transfer coefficient, Btu/hr-ft^2
H	enthalpy, Btu/lb_m
J	conversion factor, 778 (ft-lb_f)/Btu
k_e	thermal conductivity of formation, Btu/hr-ft-^{0}F
L_R	relaxation parameter defined by Eq.13, ft^{-1}
P	pressure, psia
q	volumetric flow rate, STB/D
Q	heat loss/gain, Btu/sec
Re	Reynolds number
R_s	solution gas-oil ratio, SCF/STB
s	saturation
s_o	oil saturation
s_w	water saturation

r_t	tubing radius, ft
T_f	fluid temperature, ^{0}F
T_D	dimensionless temperature
T_{ei}	reservoir temperature at depth of section 'i'
U_t	overall heat transfer coefficient, Btu/hr-ft^2-^{0}F
v	in-situ velocity, ft/s
w	mass flow rate, lb/sec
z	depth
α	angle of inclination of well, rad
β	volume expansivity, 1/^{0}R
γ_g	specific gas gravity
γ_o	specific oil gravity
σ	Joule Thomson throttling coefficient, Btu/lb$_m$-psi
μ_o	oil viscosity, cp
μ_{od}	dead oil viscosity, cp
ρ	density, lbm/ft^3
φ	lumped parameter defined by Eq. 16, ^{0}F/ft
$\emptyset$	porosity
Ψ	lumped parameter defined by Eq. 14, ^{0}F/ft

TABLE OF CONTENTS

Page

LIST OF FIGURES

Page

LIST OF TABLES

Page

CHAPTER I

INTRODUCTION

1.1 Introduction and Literature Review

Well monitoring and surveillance is critical in deep water assets as it is in shallow onshore wells. The difficulty of well monitoring is significantly higher in deep water wells as production logging and other methods of flow measurement are not very practical for use in these purposes. These deep water wells may more often than not, pass through multiple pay zones interspersed with non-producing zones. Furthermore, production logs provide information intermittently and not continuously. Well test separators and multiphase meters measure periodically or when on demand as they are generally shared among a number of wells. The periodic measurement would not be a problem for conventional reservoirs with nearly steady state production where infrequent well testing information would be enough for monitoring well performance and making business decisions. However, that is generally not the case in deep water assets with multiple pay zones where the production may fall drastically in one zone while it may remain steady in another zone or may even produce in transient state for a long period of time.

One way to monitor the production or the well is through temperature measurements. Temperature readings are considered more reliable since it takes time to dissipate thereby representing the behavior of the production for a longer period. In recent years, sensors have been developed that provide temperature measurement accurate to the nearest

0.001^0C. Distributed temperature sensors (DTS) systems have been developed which could provide temperature measurements at multiple points in the well in contrast to temperature logging which provides temperature measurement at a single point. These sensors generally do not affect the flow and can be installed more easily in restricted environment. Ouyang & Belanger (2004) found that these DTS systems could be used to accurately generate a flow profile for single phase fluid and in some cases for multiphase fluid with the help of supplemental data such as pressure measurements and holdup. These may be obtained through technologies such as DPS (distributed pressure sensors) and holdup sensors (Ouyang & Belanger, 2004).

Brown et al. (2005) described the use of DTS in combination with production logging tools to monitor production in Azeri Field. Their goal was to cut cost due to well surveillance and to not disturb the high production in the early years of the well due to production logging. Also access to wellhead was limited during drilling operations. Through the use of DTS they were able to determine the zones which contributed the most to the overall production (Brown, Field, Davies, Collins, & Garayeva, 2005).

Johnson et al. (2006) used DTS technology to estimate production from different zones using a data acquisition system, a wellbore simulator and an analysis technique. They used a trial and error approach where they matched the simulated temperature profile and actual data collected in depth domain. They then compared the flow profile with the results from production logging surveys (Johnson, Sierra, Kaura, & Gualtieri, 2006). Nath et al. (2006) discussed the use of DTS in flow profiling, in monitoring water breakthrough in horizontal

well and in monitoring fracture height (Nath, Finley, Kaura, B.Krismartopo, & Yudhiarto, 2006).

Bremer et al. (2010) used fiber optic pressure and temperature sensors for use in geothermal wells. They evaluated the sensors at different temperatures by measuring the pressures and validated the performance of the sensors using data from available literature (Bremer, et al., 2010).

Wang, Bussear & Hasan (2010) discussed the use of DTS for improving flow profiling. They applied Fourier Series to approximate DTS traces and used Solver in excel to find the coefficients of Fourier series to reduce error between DTS traces and approximation. They also used an iterative procedure and integrated multipoint pressure data with DTS data. Their techniques seemed to work well for gas wells concluding that these techniques may also work well for any well for flow profiling (Wang, Bussear, & Hasan, 2010).

A number of devices have been developed and used for production monitoring. Lenn et al. (1998) developed an integrated production logging tool that would measure fluid phase velocities, holdups, flow rates and formation saturation for horizontal wells. It would also take into account the different flow regimes in horizontal wells (Lenn, Kuchuk, Rounce, & Hook, 1998). Webster et al. (2006) developed a Venturi densitometer flowmeter that imparts flow information and detects problems on the well based on mixture density. The device is a combination of a Venturi and a gamma ray densitometer that measures mixture density (Webster, Richardson, C.Gabard-Cuoq, Fitzgerald, & Stephenson, 2006). Other tools have been developed to obtain real time flow monitoring such as Shell's

PRODUCTION UNIVERSE tool. However, this tool also relies on flow measured from test separators or multiphase meters (Poulisse, Overschee, J.Briers, C.Moncur, & Goh, 2006).

Champion (2006) described the use and principal of wireless gauge technology to obtain real time reservoir pressure and temperature data. This technique uses electromagnetic (EM) through-tubing technology. For this technology to work efficiently there must be continuous electrical conduction from the location at which pressure or temperature is being measured to the surface where the signals are received. One advantage of the wireless EM technology as described by Champion et al (2009 & 2015) is that it is not influenced by cemented casings, cement plugs or bridge plugs. They also described their successful use of EM technology in two deep water wells where there was no Christmas tree or completion string installed in the wells (Champion, 2006; Champion, Strong, & Moodie, 2009; Champion & Puntel, 2015)

In this study we use temperature and pressure measurements from different points in the production tubing for both production and injection to perform energy balances. Energy balances are performed in each producing and non-producing zone as outlined by Hasan & Kabir (2002). The energy balance takes into account all the major sources of heat transfer in the wellbore. Through a systematic procedure, the production or injection in each zone is calculated by a reverse modelling to develop a model to obtain a continuous flow profile. Thus, the zonal flow contributions for each of the producing zones can be estimated.

Estimating the zonal flow contributions could significantly help in making workover decisions and in well surveillance especially in deep water wells where production logging is difficult and would affect the performance of the well. Successful interpretation of the flow from each zone could impact the performance throughout the life of the well. The development of the model for flow profiling is discussed in the next chapter.

1.2 Research Objective

Well monitoring and surveillance comes with many difficulties in deep-water wells. Proper well monitoring is vital for well interventions. It may cost more than a million dollars for a single day during well interventions. Well interventions are operations carried out in oil and gas wells for the purpose of repair, replacement and maintenance. Well monitoring would be facilitated by continuous real time production data. However, there are rarely any flow monitoring devices that would provide such data. There are on the other hand temperature and pressure sensor devices that have been developed and are being updated which could provide continuous real time temperature and pressure measurements. A model to estimate a flow profile using temperature and pressure data could be a very useful tool in well monitoring.

The focus of this study is to develop a model for estimating production from individual pay zones in deep water wells using pressure and temperature data. An energy and momentum balance was applied to each producing and non-producing sections of the wellbore. A reverse calculation was then used to develop the final model. The model can be applied to single-phase oil reservoir as well as two-phase oil and gas wells. The change

in temperature and pressure data along the wellbore has also been taken into account for evaluating the reservoir fluid properties. Initially synthetic data was used to test the model. Finally the model developed was validated using field data of two phase fluid flow.

Sensitivity analysis was performed on both the cases under investigation that provided a better understanding of the contributions of each of the parameters involved in the model. It also demonstrated the extent of the acceptable error for each of the parameters used in the model highlighting the critical parameters of the model.

CHAPTER II

MODEL DEVELOPMENT

In this chapter, we will develop the models for estimating flow rates from various zones from temperature and pressure data. The model accounts for fluid flow and heat transfer in the wellbore. Therefore, we first describe the system through which the fluid flows, followed by assumptions made to develop the models.

2.1 The Wellbore System

The wellbore system consists of multiple pay zones. In each pay zone (producing zone), flow occurs radially in the reservoir and axially once it is inside the wellbore. In the non-producing zone, flow occurs only vertically in z-direction. The flowing fluid along the wellbore is unsaturated single-phase oil.

Fig. 1 shows a schematic of the wellbore system with alternating producing and non-producing zones. The total production is a result of the total flow occurring radially in the producing zones. This type of alternating flow and no-flow zones are characteristic of deep water assets.

The aim of this study is to estimate flow contributions from each pay zone using temperature and pressure data along the wellbore.

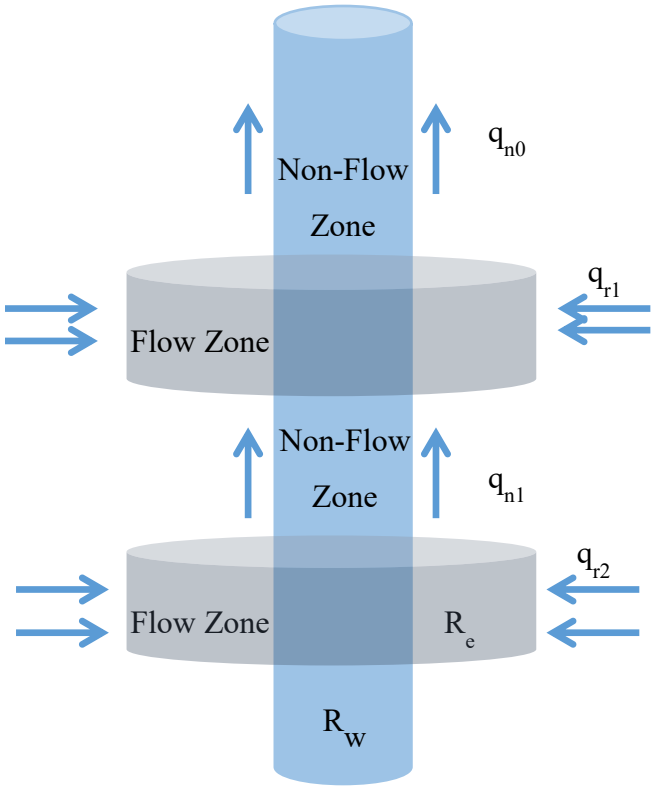

Fig. 1: Schematic of the wellbore system in the study

2.2 Model Assumptions

We are making a number of simplifying assumptions to develop the models. For example, we assume that the reservoir is homogenous, that is, all the reservoir properties are the same across the reservoir. However, the fluid properties such as density, viscosity etc. changes along the length of the wellbore as the temperature and pressure changes. Steady state conditions are assumed throughout all the pay zones. Other general assumptions are listed below:

1. Each pay zone produces at a constant rate.

2. Density and viscosity at any depth in the wellbore remains constant but changes with depth.
3. Specific heat capacity is constant throughout the wellbore.
4. Formation temperature and pressure remains constant throughout production.
5. The fluid entering the wellbore radially mixes with the fluid coming from the non-producing zone just below it to constitute the fluid in the non-producing zone above it and it attains thermal equilibrium.
6. For deep wells in high pressure reservoirs, fluid temperature may change as it flows through the reservoir towards the wellbore. This change in fluid temperature, due to fluid expansion, has been accounted for by using an available analytical expression discussed later.

We originally developed our model for single phase unsaturated oil which does not undergo any phase change. However, the energy balance does not change for two-phase flow. Therefore, we made some modifications afterwards to apply the model to two-phase flow as well.

2.3 Data Generation

Fluid pressure and temperature in deep water assets are generally not available. In order to validate our model, we first used the model to simulate various production situations and generated data. Pressure and temperature of fluid in the wellbore depend on a number of variables including the flow rate. A set of pressure and temperature data were generated

using given inflow rates in each pay zone. This data set was then used to verify the model for estimating the flow along the wellbore. We also used a set of available field data to further validate the model.

2.3.1 Pressure Calculation

We start from a point in the top most non-producing zone where the pressure in the wellbore is a given, say P_i and the total flow can be calculated from surface production data. For generating a set of pressure data, the flow rates in each non-producing zone are assumed given. Starting with the given pressure and formation temperature data the properties of the producing fluid are calculated. Properties of the producing fluid such as oil formation volume factor, solution gas-oil ratio, viscosity and density vary with temperature and pressure. These properties are then used to obtain a series of pressure data at every twenty feet by calculating pressure differential at regular intervals by applying momentum balance. The methods and correlations used for determining these properties are shown in detail in Appendix A.

Total pressure drop in the wellbore due to friction head, hydrostatic head and kinetic energy,

$$\left(\frac{dp}{dz}\right)_{total} = \frac{f\rho v^2}{2g_c} + \frac{g}{g_c}\rho sin\alpha + \rho v\frac{dv}{dz} \quad (1)$$

where f is the friction factor, ρ is the density of fluid, v is the in-situ velocity of fluid, α is the angle of inclination of the well and dv/dz is the velocity gradient,

Pressure at a point Δz below the initial point using Eular's approximation for d*p*/dz,

$$P_{i+1} = P_i + \Delta z \left(\frac{dp}{dz}\right)_{total} \quad (2)$$

Accuracy can be improved using the average value of the gradient. However, because we are using very short (20 ft) depth steps and because pressure gradient variation with depth for single-phase liquid is very small, we are using Eq. 2 without any modification.

Our model requires estimates of fluid temperature and pressure in the non-flow zones (T_n and p_n) as well as sandface fluid temperature given reservoir temperature at a given depth. Computations for these are briefly described below.

2.3.2 Temperature Calculation

For generating the temperature data we require three separate computations. These needed computations include (1) temperature of the flowing fluid along the non-producing zone; (2) temperature of the fluid entering the wellbore from the reservoir in the producing zones, and (3) temperature at the edge of each non-producing zone. For generating temperature along the wellbore in the non-flow zone, we used the Hasan-Kabir (Hasan and Kabir 2002) approach. For the temperature of the fluid entering the wellbore we applied the analytical expression given by Chevarunotaiet al. (2015), as is discussed in a later section. Finally, for calculating the temperature at the edge of each no-flow zone we applied mass and energy balance among two successive non-producing zones and the producing zone between them.

Non-producing Zone Temperature

Hasan -Kabir has shown that the temperature gradient of fluid in the wellbore can be expressed as

$$\frac{dT_f}{dz} = C_J \frac{dp}{dz} + \frac{1}{c_p}\left[-\frac{Q}{w} + \frac{g sin\alpha}{g_c} - v\frac{dv}{dz}\right] \quad (3)$$

where C_J is the Joule-Thompson (J-T) coefficient which will be discussed in a later section, c_p is the mean heat capacity of the of the fluid at constant pressure and w is mass flow rate of producing fluid.

In Eq. 3, Q accounts for heat flow rate between the reservoir and the wellbore per unit length of the well.

$$Q = -L_R w c_p\left(T_f - T_{ei}\right) \quad (4)$$

where T_{ei} is the formation temperature and L_R is the relaxation length parameter expressed as

$$L_R \equiv \frac{2\pi}{c_p w}\left[\frac{r_t U_t k_e}{k_e + (r_t U_t T_D)}\right] \quad (5)$$

where r_t is the outer diameter of tubing, U_t is the overall heat transfer coefficient, k_e is the thermal conductivity of the formation and T_D is the dimensionless temperature.

Eq. 3 is often solved with the boundary condition that fluid temperature at the well bottom, where reservoir fluid enters the wellbore, is the same as the undisturbed reservoir temperature. This, however, is untrue for high draw down and high flow rate systems, and

is never true where fluid from various zones at different temperatures comingle together. In those cases, Hasan et al. (2009) solved Eq. 3 by dividing the wellbore in various sections and using the fluid entrance temperature at each section as the boundary condition for each section. For our system, that is the appropriate solution, which is given by,

$$T_f = T_{ei} + \frac{1 - e^{(z-z_l)L_R}}{L_R}\Psi + e^{(z-z_l)L_R}\left(T_{fi} - T_{ei\,j}\right) \tag{6}$$

where,

$$\Psi = \left[g_G \sin\alpha + \varphi - \frac{g \sin\alpha}{c_p}\right] \tag{7}$$

$$\varphi = C_J \frac{dp}{dz} - \frac{v}{c_p}\frac{dv}{dz} \tag{8}$$

In Eq. 6 T_{fi} is the temperature of the fluid at bottom of each non-producing section and T_{eij} is the temperature of the formation at this depth. The last term on the right hand side of Eq. 6 accounts for difference in the temperature of fluid in the bottomhole and that of the formation.

Note that the second term on the right hand side of Eq. 8 may be ignored for single phase unsaturated oil. The term *dv/dz* would be very small because liquids are only slightly compressible.

When calculating L_R, all the parameters on the left hand side of Eq. 5 may not be available. In such cases the following approach may be used for L_R computation,

$$L_R = \frac{L_{R,const}}{q} \tag{9}$$

where $L_{R,const}$ is a constant. For single phase liquid, expression for J-T coefficient that may be used,

$$C_J = -\frac{1 - T_{ei}\beta}{c_p \rho} \tag{10}$$

where $=T_{ei}$ is in ^{0}R and β in $1/^0$R is the volume expansivity.

Zonal Contribution Estimation

These set of equations can be used to obtain a temperature profile for each non-producing zone. Fig. 2 can be used to clarify the procedure for calculating temperature in each zone. Subscript *n* implies non-flow zone and subscript *i* implies reservoir quantities. If zone 2 is the last zone, then T_{n2i}, fluid temperature at the bottom of this non-flow section, is the same as the reservoir fluid entering here. The temperature of the fluid entering wellbore from the reservoir is calculated from the reservoir temperature at this depth and using Chevarunotai's analytical solution to account for J-T heating. T_{n2j}, which is the temperature at the top edge of this non-producing zone is calculated from T_{n2i} using Eq. 6. $T_{r,avg1}$ and $T_{r,avg2}$ are the average temperature of the reservoir fluid entering the wellbore for this section. As before, these temperatures are calculated from the reservoir temperature at this depth and using Chevarunotai's equation. Now the temperature at the bottom edge of the next non-producing zone, that is, T_{n1j} is calculated from an energy balance in zone 1, zone 2 and the producing zone in between. This method is repeated in all the following zones.

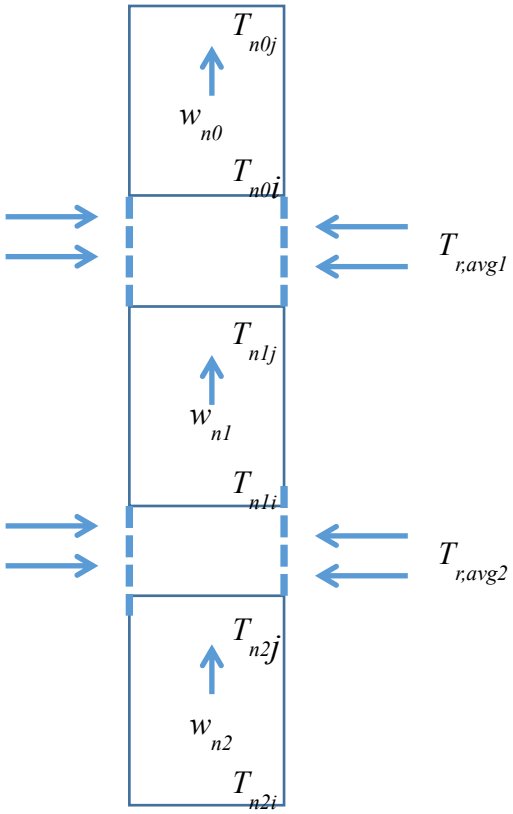

Fig. 2: Temperature distribution in the wellbore system

Sandface Fluid Temperature

For determining the temperature of the flowing fluid at the edge of each non-producing zone we perform energy and material balances. One of the parameters required in this energy balance is the average temperature of the fluid flowing radially in the wellbore from the reservoir. This temperature is not necessarily the same as the temperature of the reservoir at that depth. In reservoirs with high pressure drawdown, as the fluid moves from a very high pressure towards the wellbore, the lowering of pressure causes the fluid to expand and thus changes its temperature. In deep reservoirs with high drawdown this

change in temperature is significant and should be accounted for. We applied the analytical model by Chevarunotai et al. (2015) to estimate temperature in the producing zones for such reservoirs. This analytical model takes into account the Joule Thompson effect which is a phenomenon where temperature of the fluid changes due to expansion of the fluid at constant enthalpy without production of work or transfer of heat. The expression for the flowing fluid temperature in the reservoir, incorporating heat transfer between the system and the surroundings is given by Chevarunotai et al as

$$T(r,t) = T_{ei} + \frac{C}{2B} e^{\frac{H(Ar^2+2Bt)}{2B}} Ei\left[-\frac{H(Ar^2+2Bt)}{2B}\right] - \frac{C}{2B} e^{\frac{HAr^2}{2B}} Ei\left[-\frac{HAr^2}{2B}\right] \quad (11)$$

where

$$A = \left[\emptyset s_o \rho_o c_{po} + \emptyset s_w \rho_w c_{pw} + (1-\emptyset)\rho_f c_{pf}\right]\left(\frac{2\pi h}{q}\right) \quad (12)$$

$$B = \rho_o c_{po} \quad (13)$$

$$C = \frac{q\rho_o \sigma_o \mu}{2\pi h k_e} \quad (14)$$

$$H = \frac{D}{A} \quad (15)$$

$$D = \frac{4h_c \pi}{q} T_{ei} \quad (16)$$

where $\emptyset$ is the formation porosity, h is the formation thickness, h_c is the heat transfer coefficient, $\sigma_o$is the Joule Thompson throttling coefficient, s is oil or water saturation and *Ei* represents Eigen function. The subscripts *o, w,* and *f* represents oil, water and formation.

The equation for temperature is for pseudo steady state conditions and represents temperature of fluid entering the wellbore at time *t* and radius *r*.

Note that momentum and energy transport are generally coupled because property values needed for these computations are dependent on both pressure and temperature. However, the effects of temperature on transport properties are very small. Therefore, we calculate the pressure profile first, starting from the known pressure above all perforations, and we work our way down to the bottom of the well. Thus, when generating temperature data, the pressure and flow rate data are available, so that this is not an iterative calculation. On the other hand, the temperature calculation begins at the bottom of the very last non-producing zone (that is, the bottom of the well) and we work our way up to the wellhead.

2.4 Single Phase Flow Profile from Energy Balance

To obtain an expression for flow rate at any non producing zone we set up an energy balance for the controlled volume as shown in Fig. 3. We use subscripts n and r to represent quantities in the non-producing zone and the reservoir, respectively. The fluid coming from the reservoir at a rate of w_{r1} (lb/day) at a temperature T_{r1}, mixes with the fluid coming from the lower non-producing zone at a rate of w_{n1} (lb/day) at a temperature T_{n1}. The mixed fluid enters the upper non-producing zone and has the rate w_{no} (lb/day) and temperature T_{no}.

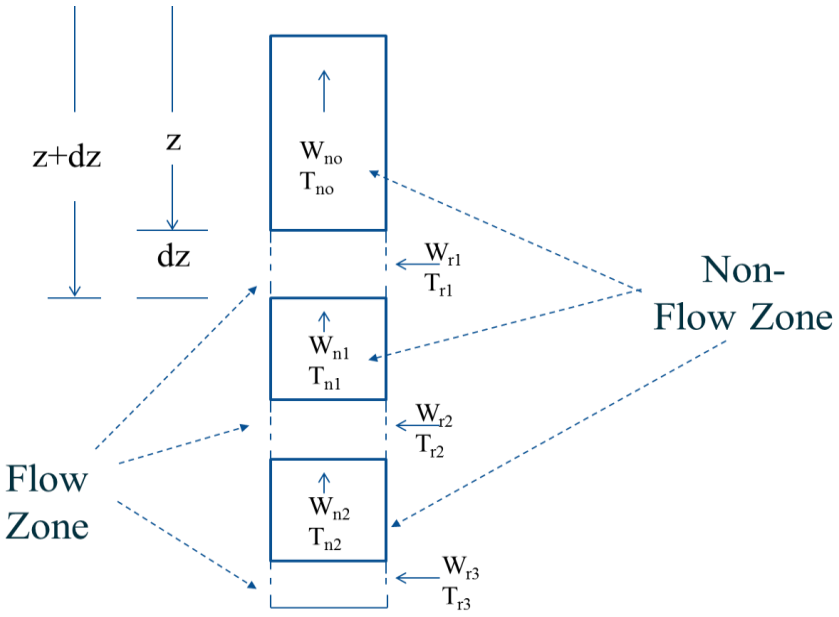

Fig. 3: Alternating producing and non-producing zones

Consider a control volume inclined at an angle α to the horizontal having a length dz at a distance z from the surface. An energy balance for the system including potential and kinetic energies to the enthalpy of the fluid would be as follows.

$$w_{n1}H|_{z+dz} - \frac{(z+dz)w_{n1}g\sin\alpha}{Jg_c} + \frac{w_{n1}v^2|_{z+dz}}{2Jg_c} + Qdz + w_{r1}H_r|_{z+dz} + \frac{w_{r1}v_r^2|_{z+dz}}{2Jg_c} =$$

$$w_{n1}H|_z - \frac{zw_{n1}g\sin\alpha}{Jg_c} + \frac{w_{n1}v^2|_z}{2Jg_c} + w_{r1}H_r|_z - \frac{w_{r1}gdz\sin\alpha}{Jg_c} + \frac{w_{r1}v_r^2|_z}{2Jg_c} \qquad (17)$$

In Eq.17 the terms $w_{n1}H|_{z+dz}$ and $w_{r1}H_r|_{z+dz}$ represents the enthalpies of fluids w_{n1} (lb/day) and w_{r1} (lb/day) entering the control volume through convection of fluid coming from the non-producing zone and from the reservoir respectively. Qdz represents the amount of heat

added to the control volume through conduction from the reservoir. Similarly, ($w_{no}H|_z$) enthalpy leaves the element at z by convection. Note that w_{no} is the mass flow rate of the mixed (total) fluid and equals $w_{n1} + w_{r1}$ and H_{no} represents the enthalpy of the mixed fluid. The terms $\frac{w_{n1}v^2|_{z+dz}}{2Jg_c}$ and $\frac{w_{r1}v_r^2|_{z+dz}}{2Jg_c}$ represent the kinetic energies of the fluid. Contribution of radial kinetic energy terms in the energy balance equation is negligible compared to other energy terms and hence these terms are neglected. The second terms on both the left and right hand side represent the potential energy of the flowing fluids.

In Eq. 17, g_c and J represent conversion factors, g_c = 32.2 (lb_m-ft)/(lb_f-s^2) and J = 778 (ft-lb_f)/Btu. Note that for a given zone, the reservoir fluid is coming from various elevations to the non-producing zone n_o; we use an arithmetic average (half) of the potential energy.

For the first part of our study, the flowing fluid does not undergo any phase change. Therefore, there are negligible heat effects due to phase change, condensation, solution or mixing. In such conditions, enthalpy change is a function of pressure and temperature

$$dH = c_p dT - C_J c_p dp \tag{18}$$

In addition, as shown previously, the heat exchange between the formation and wellbore fluid, Q, can be expressed as,

$$Q = -L_r w c_p (T_{no} - T_{ei}) \tag{19}$$

Thus, combining Eq.17, Eq.18 and Eq.19, we get,

$$w_{n1}c_{p1}\left((T_{n0}-T_{n1})-C_J(p_{n0}-p_{n1})-\frac{\Delta z g\sin\alpha}{c_{p1}Jg_c}\right)+\ w_{r1}c_{pr}\left((T_{n0}-T_{r,avg})-\right.$$

$$\left.C_J(p_{n0}-p_{r,avg})-\frac{\Delta z_{avg}g\sin\alpha}{c_{pr}Jg_c}\right)=L_r(w_{n1}c_{p1}+w_{r1}c_{pr})(T_{n0}-T_{ei}) \quad (20)$$

Now from mass balance,

$$w_{r1}=w_{no}-w_{n1} \quad (21)$$

w_{no} is a known quantity from surface production data. Combining Eq. 20 and Eq. 21 and assuming $c_{p1}=c_{pr},\ \Delta z_{avg}=\frac{1}{2}\Delta z$, and that there is no addition of heat from the formation, that is, $Qdz=0$, we arrive to an expression for flow rate in the wellbore in the non-producing section

$$w_{n1}=w_{n0}\frac{(T_{n0}-T_{r,avg})-c_J(p_{n0}-p_{r,avg})-\frac{1}{2}\frac{\Delta z g sin\alpha}{Jg_c c_p}}{(T_{n1}-T_{r,avg})-c_J(p_{n1}-p_{r,avg})-\frac{1}{2}\frac{\Delta z g sin\alpha}{Jg_c c_p}} \quad (22)$$

Generalizing this equation and taking $w_{n1}=q_{n1}\rho$ and $w_{n0}=q_{n0}\rho$,

$$q_{n(i+1)}=q_{ni}\frac{(T_{ni}-T_{r,avg})-c_J(p_{ni}-p_{r,avg})-\frac{1}{2}\frac{\Delta z g sin\alpha}{Jg_c c_p}}{(T_{n(i+1)}-T_{r,avg})-c_J(p_{n(i+1)}-p_{r,avg})-\frac{1}{2}\frac{\Delta z g sin\alpha}{Jg_c c_p}} \quad (23)$$

Starting from the top zone we can calculate $q_{n(i+1)}$and obtain a continuous flow profile. From the difference in flow rate between two consecutive non-producing zones we can find out the contribution of each producing zone to the total production.

From Eq. 23 an expression of T_{ni} can be obtained such that,

$$T_{ni} = \frac{q_{n(i+1)}}{q_{ni}}\left[T_{n(i+1)} + c_J\left(p_{ni} - p_{(i+1)}\right) + \frac{\Delta z g sin\alpha}{J g_c c_p}\right]$$

$$+ \frac{q_{ni} - q_{n(i+1)}}{q_{ni}}\left[T_{r,avg} + c_J\left(p_{ni} - p_{r,avg}\right) + \frac{1}{2}\frac{\Delta z g sin\alpha}{J g_c c_p}\right] \quad (24)$$

We used Eq. 24 to calculate the temperature of fluid at the edge of each non-producing zone (except the last zone, where Chevarunotai's analytical solution was used). Note that the T_{ni} in Eq. 24 is used as T_{fi} in Eq. 6.

Using equations for temperature in this chapter along with the equations in Appendix A, we generated a set of temperature and pressure data to test our model. We will name this set of generated data and other properties for this case study as Case I. Details for Case I are shown in Appendix B. As shown in Fig. 4 we found the forward and reverse modeling to be in perfect agreement.

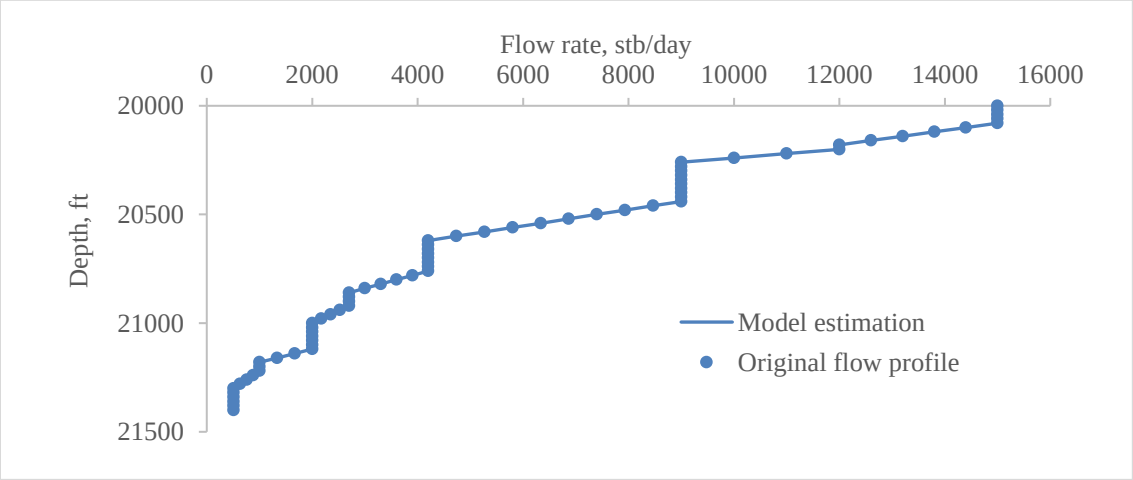

Fig. 4: Comparison of original flow profile assumed with model estimated flow profile

2.5 Model Modified for Two Phase Flow Profile

The energy balance we developed is also applicable for a two phase flow (gas and liquid, liquid constituting water and oil); hence the model developed can be extended for use in cases of two phase flow profiling. However, we would need to know the water oil ratio (WOR) and gas oil ratio (GOR) or gas liquid ratio (GLR) in addition to the other known parameters.

When dealing with two-phase flow we first calculate the mass flow rate profile rather than the volumetric flow rate profile. For the topmost non-producing zone this can be calculated from total production data such that,

$$w_{no} = (q_o\rho_o + q_w\rho_w)5.615 + (q_o + q_w)\gamma_g GLR \times 0.0765 \tag{25}$$

The mass flow rates in the following non-producing zones can then be calculated from the generalized form of Eq. 22, that is,

$$w_{n(i+1)} = w_{ni}\frac{(T_{ni} - T_{r,avg}) - c_J(p_{ni} - p_{r,avg}) - \frac{1}{2}\frac{\Delta z g sin\alpha}{Jg_c c_p}}{(T_{n(i+1)} - T_{r,avg}) - c_J(p_{n(i+1)} - p_{r,avg}) - \frac{1}{2}\frac{\Delta z g sin\alpha}{Jg_c c_p}} \tag{26}$$

where $w_{n(i+1)}$ is in lb/day. Next we can obtain the flow rates in STB/d in the following zones as follows,

$$q_{oi} = \frac{w_{ni}}{5.615(\rho_o + \rho_w WOR) + 0.0765\gamma_g GLR(1 + WOR)} \tag{27}$$

$$q_{wi} = WOR\,q_{oi} \tag{28}$$

$$q_{gi} = (q_{oi} + q_{wi})GLR \quad (29)$$

We applied this approach to validate our model using a set of field data as described in the next chapter.

2.6 Flow Estimation for Injection

When applying the model for injection, at first glance it would seem that the model is also applicable for estimating flow profile for injection. However, the difference in the energy balance between production and injection is that the temperature of the fluid flowing out of the wellbore has the same temperature as the fluid from the non-producing tube preceding it. In case of production, this would have the temperature of the fluid flowing from the reservoir to the wellbore, which could be estimated from the undisturbed reservoir temperature. Therefore, this model cannot be applied to estimate injection flow profile without further information.

CHAPTER III

MODEL APPLICATIONS AND VALIDATION

3.1 Model Applications

The model developed in Chapter II for flow rate estimation can generally be applied to both single phase unsaturated oil flow and for two phase flow. In Chapter II, we validated the model using simulated data for single-phase oil flow. In this chapter we present model validation with three-phase flow field data.

This model can also be used to generate a temperature and pressure profile along the wellbore when the flow rate in a section of the well is a known quantity. This forward calculation also allows evaluation of reservoir permeability and a good estimate of temperature of fluid entering the wellbore, as shown by the equations in chapter II. A reasonable estimate of entering fluid temperature permits a more accurate energy balance. Temperature and pressure profile can be used to better determine other fluid properties such as viscosity and density, which in turn gives us a better idea about the flowing fluid thereby, the well productivity.

3.2 Model Validation

In this study, we used fluid properties, actual well temperature, and pressure data to test the model. We validated our model using data reported by Ouyang & Belanger (2004).

Table 1 lists fluid properties and well dimensions used in this study (Ouyang and Belanger 2004).

Table 1: Wellbore dimensions and fluid properties for the system used for validating the model

Parameter	**Value, unit**
Internal tubing diameter	3 in
Outer tubing diameter	3.5 in
Reservoir outer radius	4000 ft
Pipe roughness	0.00015 ft
Wellhead pressure	600 psi
Formation temperature at surface	79^0F
Geothermal gradient	0.00966 ^{0}F/ft
Oil API gravity	40^0
Gas liquid ratio	448 SCF/STB
Specific gas gravity	0.7
Specific heat capacity	0.625 Btu/lbm-^{0}F
Thermal expansivity	0.00018 $^0F^{-1}$
Surface tension	0.06952 lbm/s^2

3.2.1 Field Production Data

The well considered is a 5000 ft long vertical well perforated at three different intervals: 2000 to 2600 ft, 2900 to 3500 ft and 4400 to 4900 ft. The inflow is uniform in each interval but is not the same for each interval. Table 2 lists the contributions of oil, water and gas production in each interval. Fig. 3.1 shows the distribution of oil and water separately in each interval.

Table 2: Fluid contribution from perforated intervals

Perforated intervals (ft)	**Oil inflow (stb/d)**	**Water inflow (stb/d)**	**Gas inflow (Mscf/d)**
2000-2600	600	0	268.8
2900-3500	1200	0	537.6
4400-4900	200	1000	537.6
Total	2000	1000	1344

Fig. 5 shows that water is only produced at the last perforated zone near the bottomhole. For applying the model, we assumed water and oil as a single phase so that this is a two-phase system with free gas.

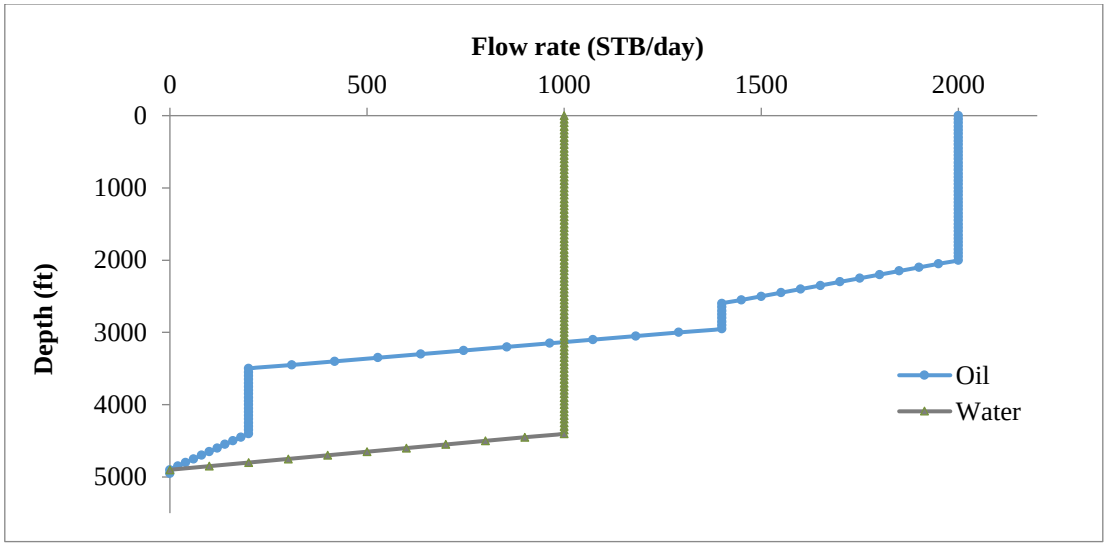

Fig. 5: Flow profile of the given well

3.2.2 Field Temperature Data

Fig. 6 shows the given formation temperature profile and wellbore temperature profile. As more fluid enters the wellbore and rate increases, wellbore temperature deviates from the formation temperature. The fluid temperature in the reservoir is affected by the Joule Thompson effect because of the significant drawdown involved. As the fluid flows in the wellbore towards the surface, the temperature of the fluid decreases due to heat loss to the lower temperature surrounding. Before applying the temperature data to our model, we first estimated the wellbore temperature profile using Eq. 6 to Eq. 8 and the given formation temperature profile. Fig. 7 shows a comparison of the given field data and our model estimated values. Both the temperature profile shows a satisfactory match.

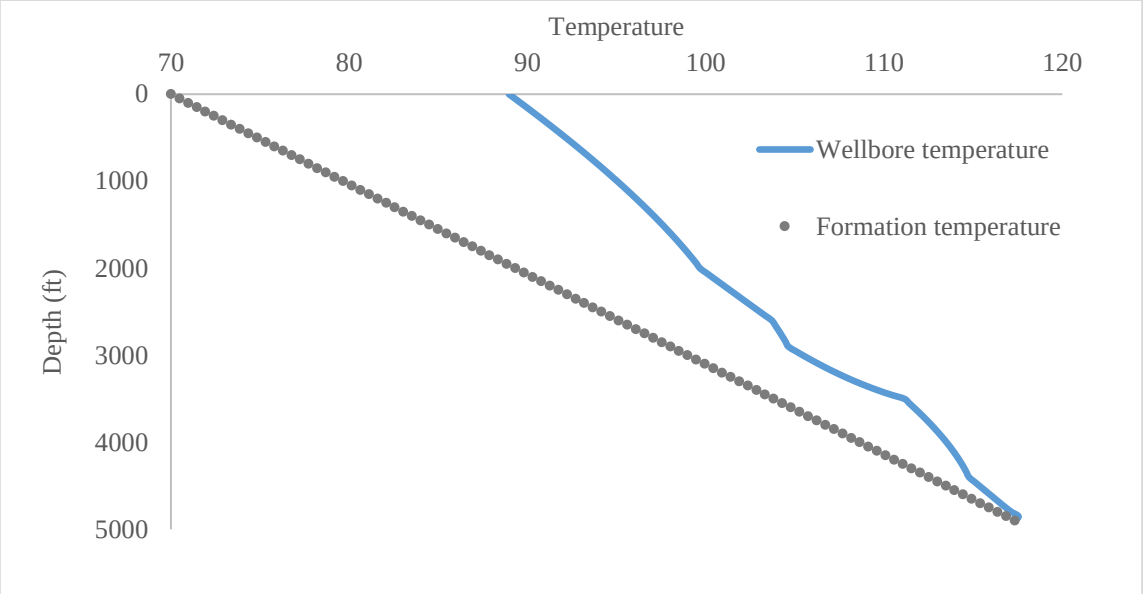

Fig. 6: Wellbore and formation temperature profile

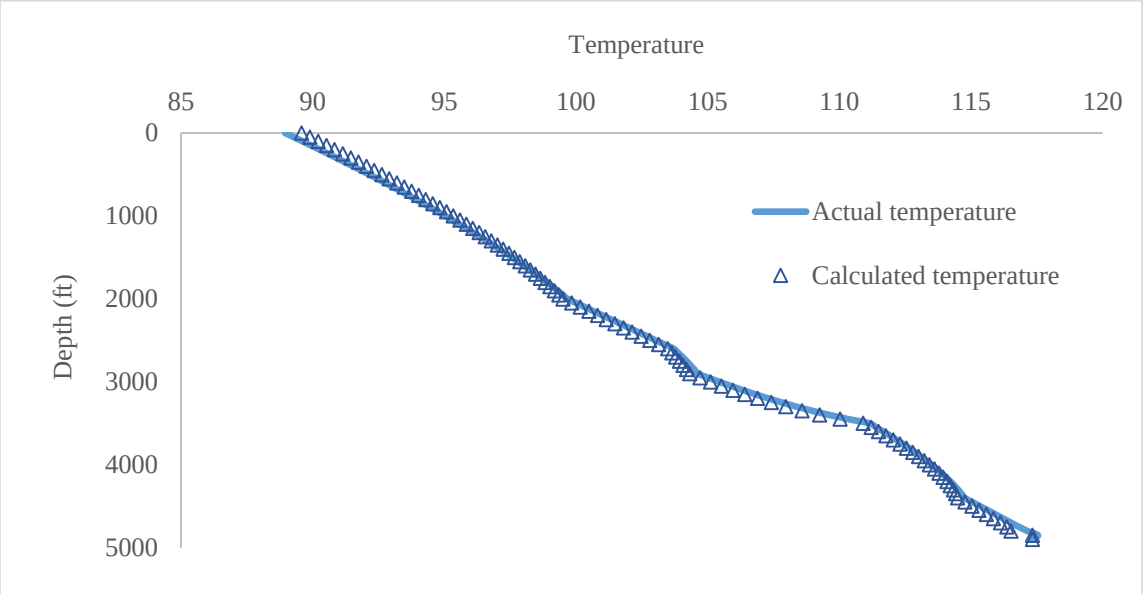

Fig. 7: Comparison of field temperature data and calculated temperature data

3.3 Model Results

We computed the flow profile for the given well described by Ouyang and Belanger (2004) by the procedures outlined in the previous chapter. Fig. 8 shows a comparison of the given production flow profile and the flow profile generated with our model using the given temperature and pressure data. These two flow profiles are in excellent agreement. We conclude that our model can therefore be applied to steady state, single phase or two-phase flow.

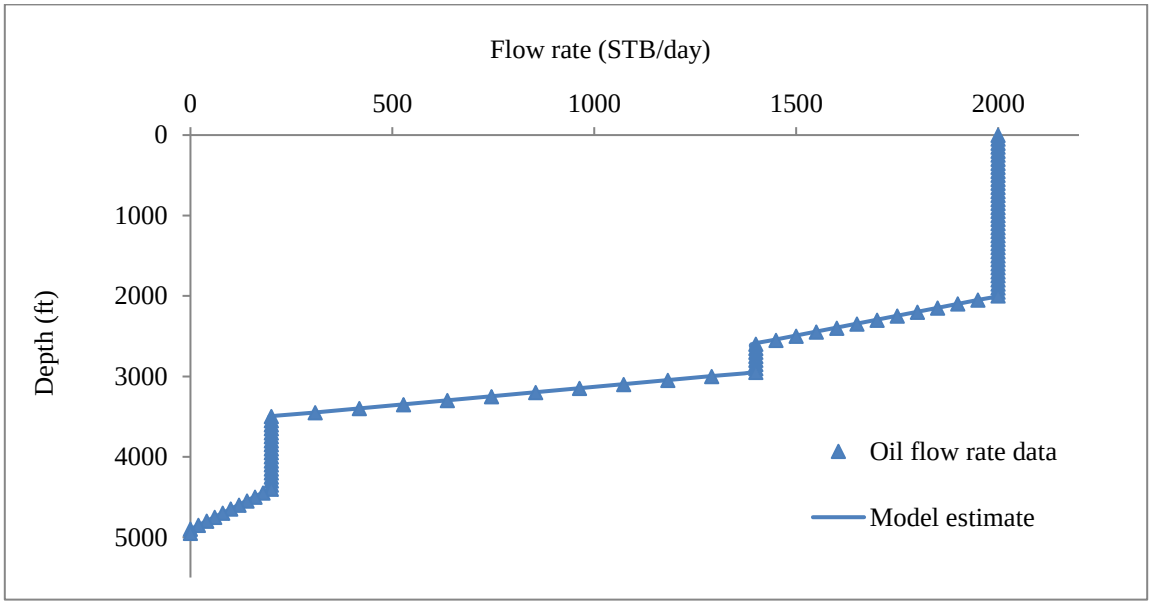

Fig. 8: Comparison between oil flow rate data and flow profile estimated using model

An important aspect of the model developed here is that it accounts for all forms of energy; in the past, that was not generally the case. Indeed, conventional production logging uses "mixing cup" approach that only accounts for fluid temperature (Hill 1990). Kabir et al.

(2011) also used the mixing cup model in their previous work (Kabir et al. 2011). In their method, the potential energy term was not taken into account in the energy balance for flow profiling. Fig. 9 shows the flow profile obtained using this former method compared to the original flow profile of the well described by Ouyang & Belanger (2004). The error is quite significant. Similarly, Fig 10 shows the errors that result if the potential energy terms are neglected for Case I where case I constitutes the synthesized data (details shown in Appendix B). Comparison of Fig. 8 and 9 clearly illustrate the inaccuracy that results when assuming negligible potential energy.

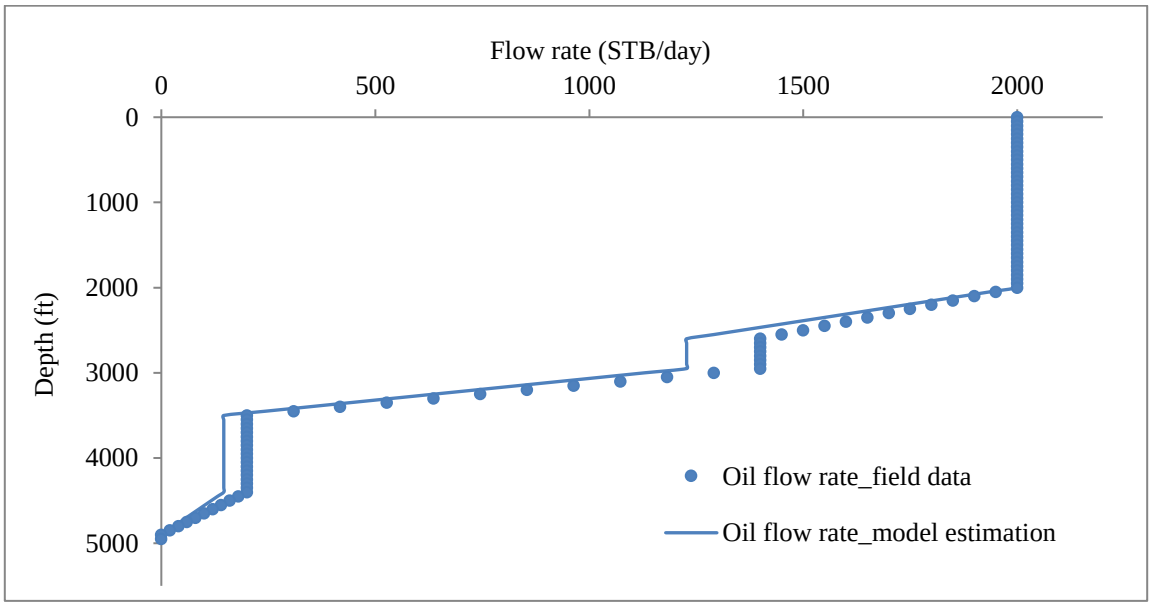

Fig. 9: Comparison between flow profile from field data and calculated flow profile neglecting potential energy term

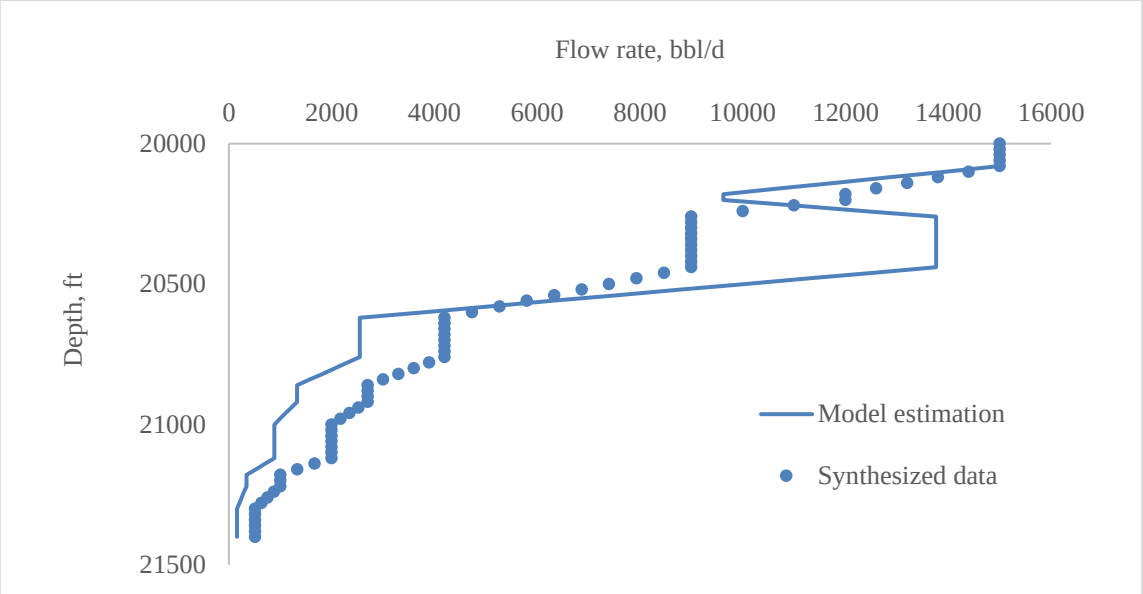

Fig. 10: Comparison between flow profile from field data and calculated flow profile neglecting potential energy term for synthesized data

CHAPTER IV

SENSITIVITY ANALYSIS

4.1 Focused Parameters

The focus of our study is to estimate flow rate from pressure and temperature data. All data come with some uncertainties. In this chapter, we will show the impact in flow rate estimation that may result from error in pressure and temperature data. However, pressure and temperature are not the only parameters involved in the flow rate estimation, a number of other parameters are also required to generate the flow profile. These parameters include, but are not limited to, well deviation, fluid properties of density, specific heat capacity, thermal expansivity, Joule-Thompson coefficient, etc.

Some of these fluid properties cannot be measured directly. Their measurement involves a number assumptions or uncertainties. A sensitivity analysis is therefore essential to understand which parameters have greater impact on flow rate estimation. This study can then be used as an incentive to gather more information on these parameters and collect more data points to obtain a reasonably accurate flow profile.

The focused parameters in our study are the temperature, pressure, density, specific heat, thermal expansivity and Joule-Thompson coefficient. All other reservoir and fluid data are as shown in Appendix B and Chapter III.

Sensitivity analysis results are shown in the next section for two base cases; case I being the synthesized reservoir condition (Appendix B) and case II being the given reservoir condition as shown in Chapter III, (Table 1&2).

The Design of experiment was then performed to show the individual and interactive effects of the critical parameters on flow profile calculation.

4.2 Sensitivity Analysis Results

We generated a flow profile from simulated pressure and temperature data. These pressure and temperature data were in turn used to reproduce those flow rates. These assumed flow rates are our original flow rates as labeled in the following plots.

We begin our study by applying error in temperature data, keeping all other factors constant. Flow profile estimation is quite sensitive to temperature as seen in Fig. 11. For Case I, a 1^0C error in temperature added throughout the wellbore results in 70% error in flow rate estimation at the bottomhole as shown in Table 5 (Appendix C). Note that these measures are for extreme cases when we assume error in temperature at every location. Thus the importance of accurate temperature cannot be overemphasized. In addition, in recent years' temperature measuring devices have been developed which provides better accuracy than 0.1^0C.

For case II the sensitivity to temperature is less than case I. 1^0C error added to the temperature throughout the wellbore results in a 9% error in flow estimation at the bottomhole as shown in Fig. 12. This is due to the lower temperatures in case II because of lower depth and other associated properties.

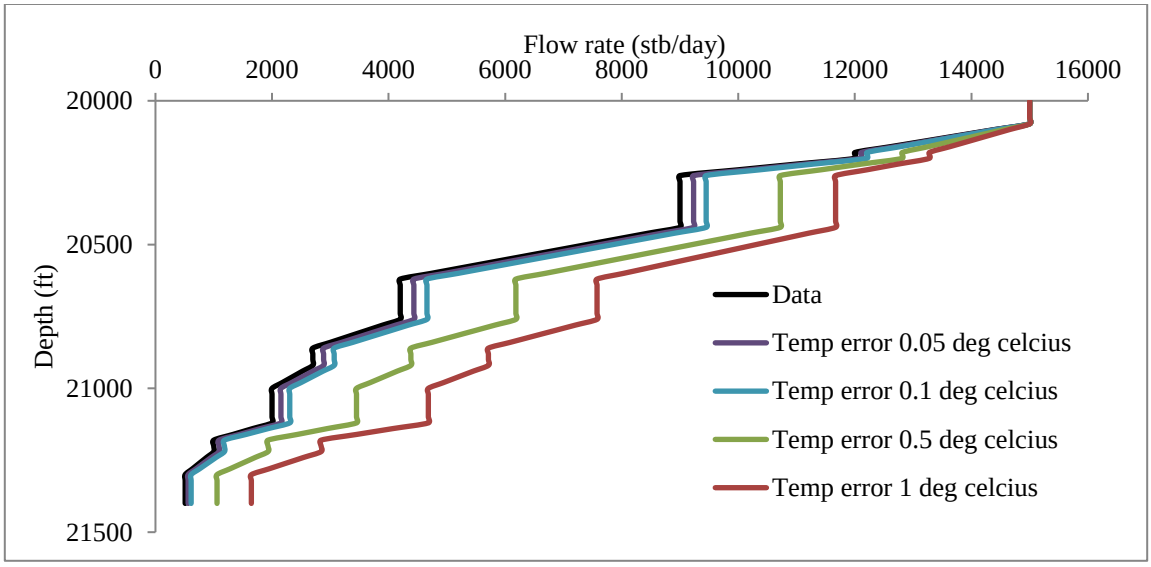

Fig. 11: A sensitivity analysis of flow profile to error in temperature data for case I

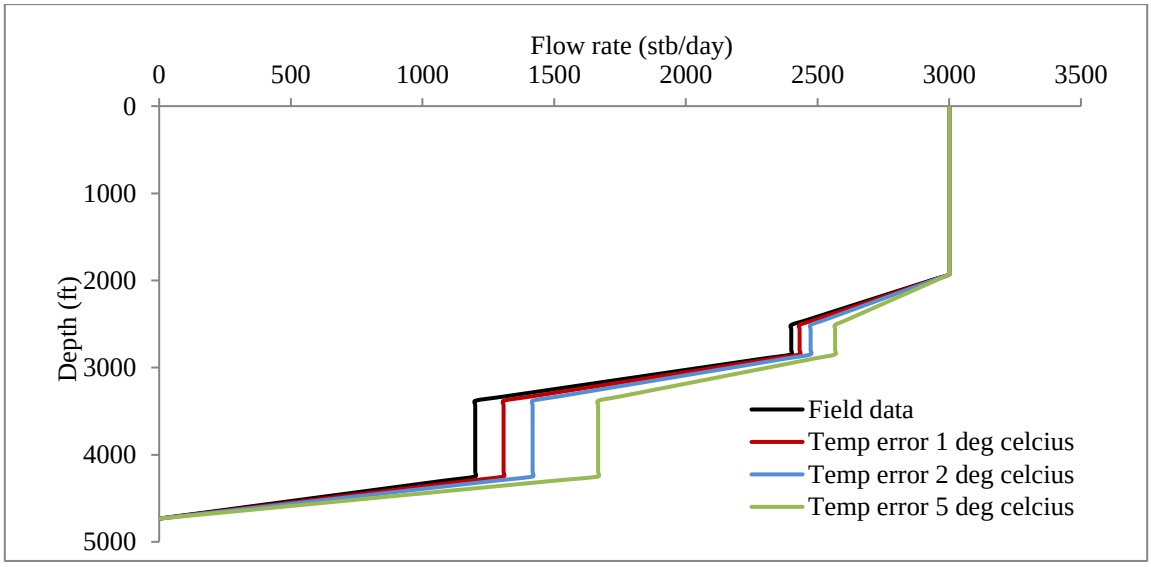

Fig. 12: A sensitivity analysis of flow profile to error in temperature data for case II

Adding error to pressure data throughout the wellbore for case I, we found the maximum error in estimation in flow rate to be about 8% (near the bottomhole) for a 10% error in the pressure data as shown in Fig. 13. Similarly, an error of 38% was observed for an added error of 40%.

The sensitivity of error in pressure data for case II is not however as great as in Case I as shown in Fig. 14. We only have a 7% underestimation in overall production at the bottom hole for a 40% error in pressure. One reason for this lower sensitivity is that there are fewer zones for case II than case I since each extra zone adds to the error. The comparison of these errors are tabulated in Table 5 (Appendix C). Note that the flow rate shown in the table is the liquid flow rate, not the overall flow rate.

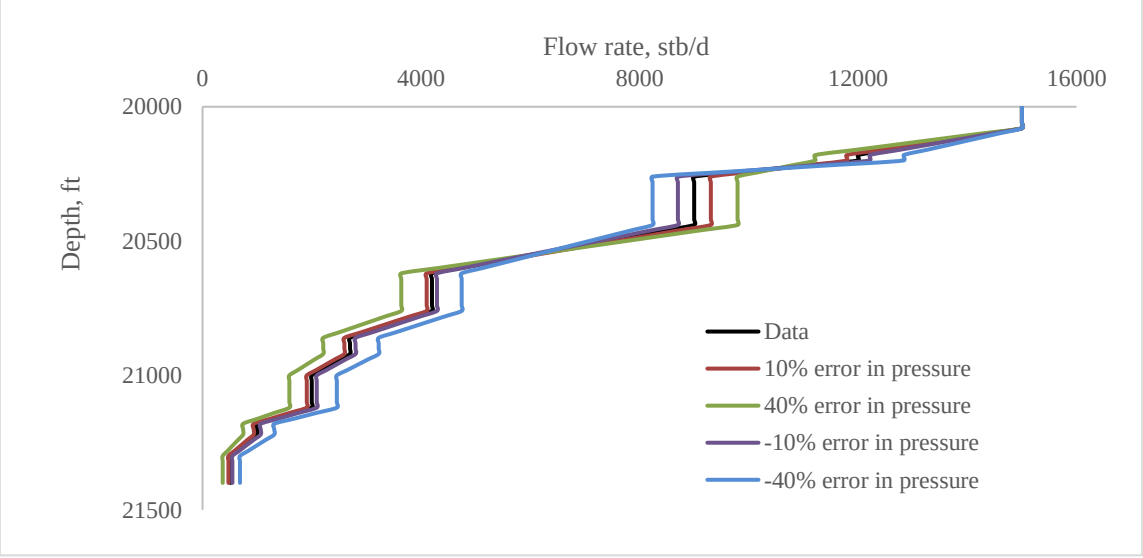

Fig. 13: A sensitivity analysis of flow profile to error in pressure data for case I

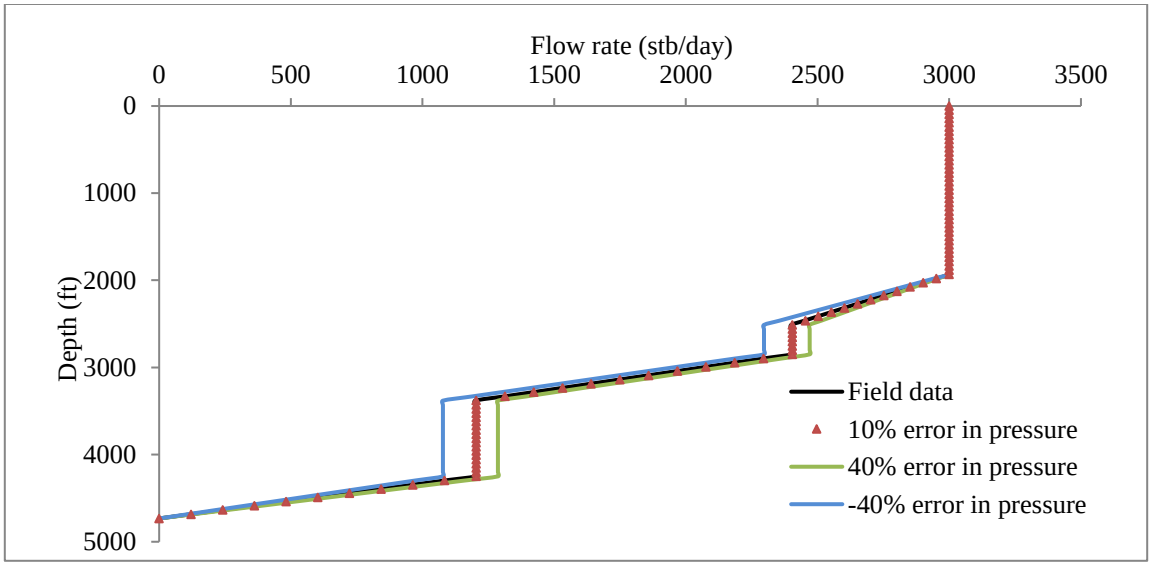

Fig. 14: A sensitivity analysis of flow profile to error in pressure data for case II

Fig 15 and Fig 16 shows that density of fluids has minor impact on flow estimation. When taking a density of almost 10 lb/ft^3 higher than the actual density we only have a 10% error in flow estimation. The plot for case I further clarifies this point by comparing the flow profiles for the original case where density is about 55 lb/ft^3 to the flow profile obtained if density is considered as high as 85lb/ft^3

The impact of density of fluid is even lower for case II where the original density is lower than in case I. In case II, the impact of density is almost half than that of case I. For a 10 lb/ft^3 higher density the error in flow rate at the bottomhole is only about 5%. Comparison of the effects of error added to density for Case I and Case II are shown in Table 7 (Appendix C).

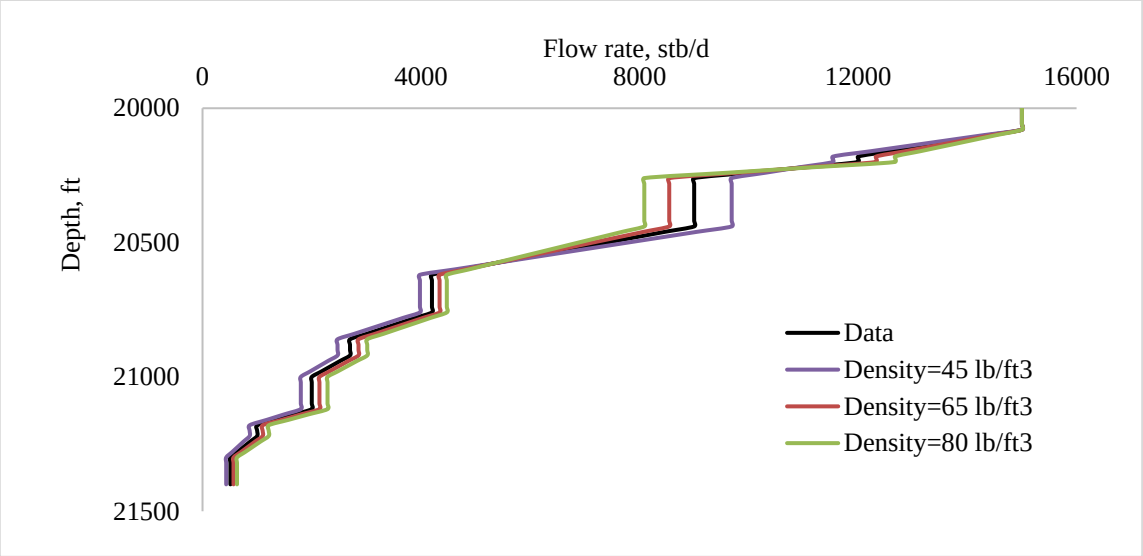

Fig. 15: A sensitivity analysis of flow profile to error in density for case I

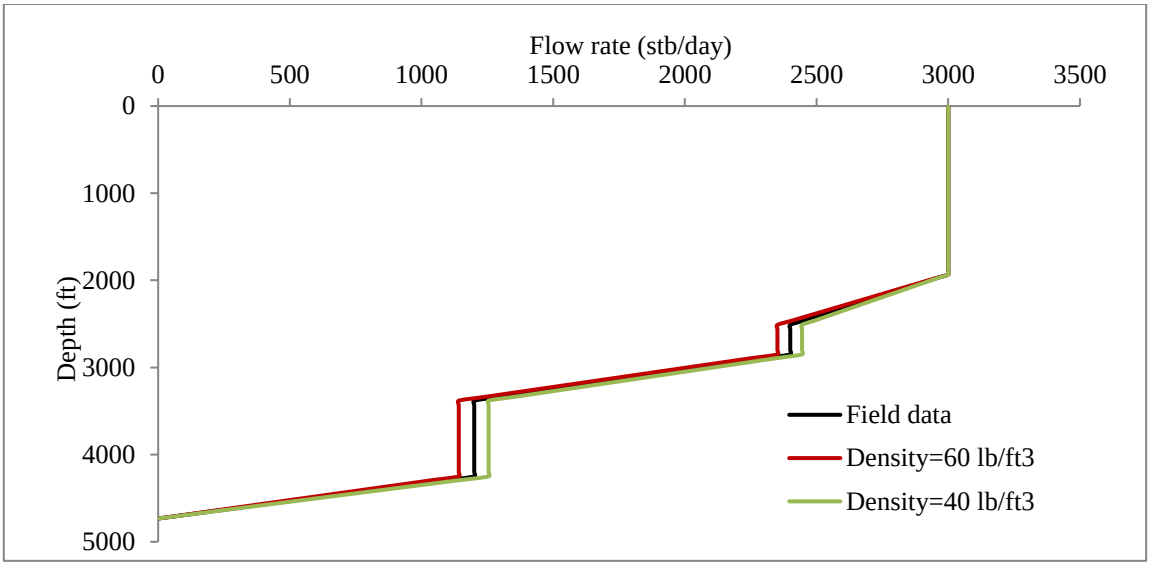

Fig. 16: A sensitivity analysis of flow profile to error in density for case II

Next, we studied the effect of specific heat on flow estimation. The sensitivities of specific heat on the flow profile are shown in Fig. 17 and Fig. 18. For both case I and II the effects of specific heat on flow rate is very small Table 8 (Appendix C). However, the extent of error in rate does not have a consistent trend. To clarify, for case I, higher values of specific heat gives lower error in flow profile whereas for case II, lower values of specific heat gives lower error in flow profile.

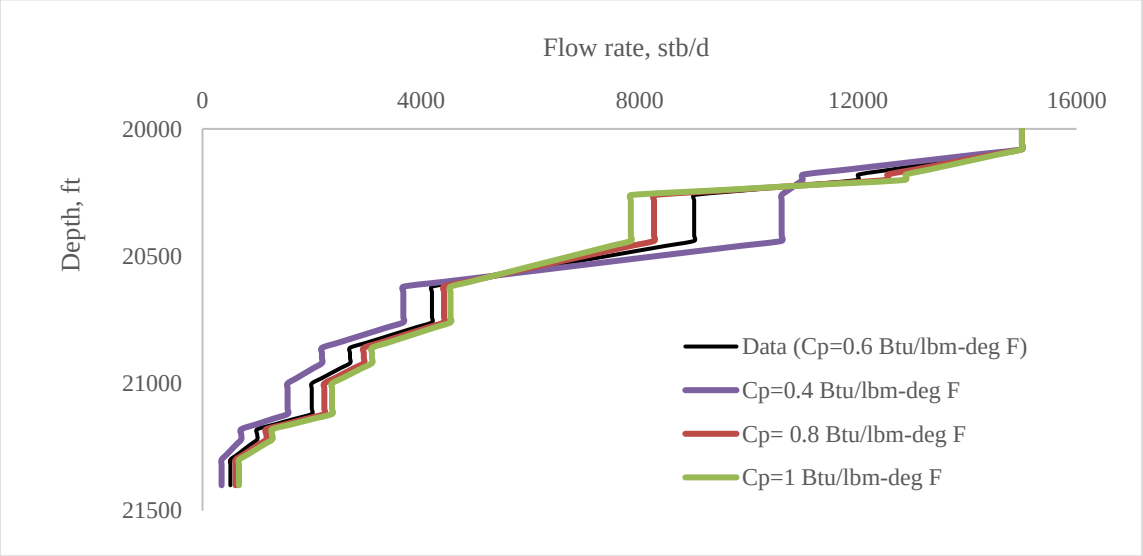

Fig. 17: A sensitivity analysis of flow profile to error in specific heat capacity for case I

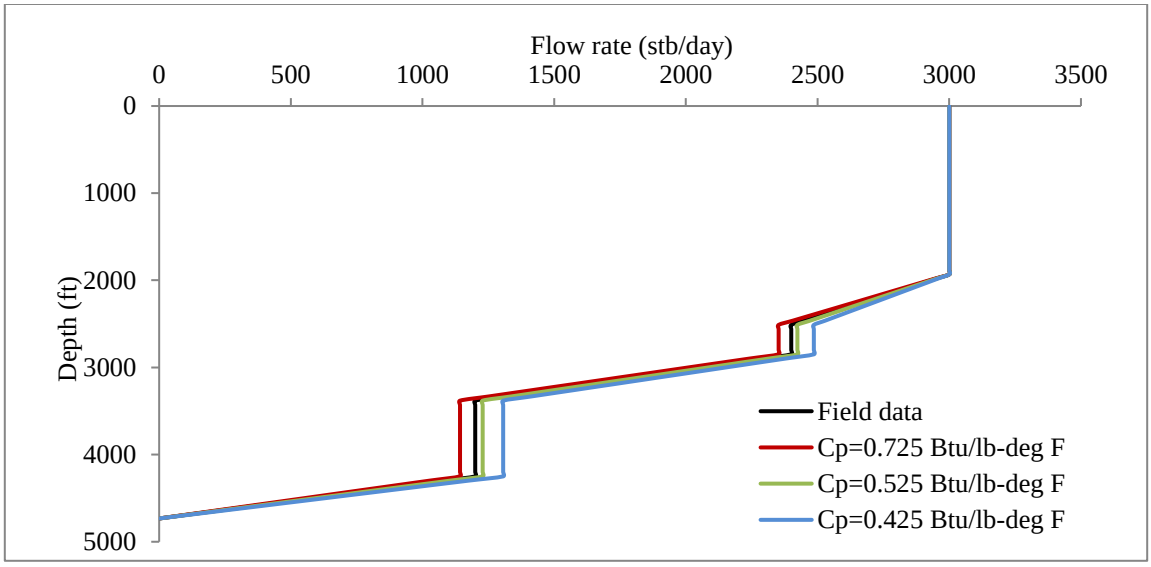

Fig. 18: A sensitivity analysis of flow profile to error in specific heat capacity for case II

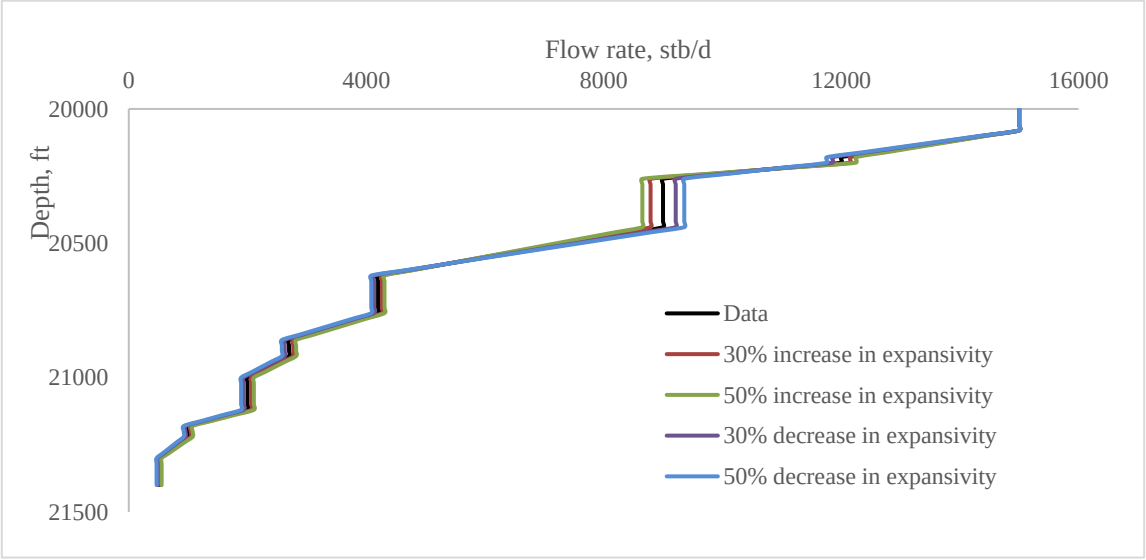

Fig. 19: A sensitivity analysis of flow profile to error in thermal expansivity for case I

Sensitivity of expansivity of fluid on flow rate is shown in Fig. 19 and Fig. 20. Effect of expansivity is quite small on flow rate. For a 30 % error in expansivity there is only a 5% error in flow rate at the bottomhole for case I and less than 4% error in flow rate for case II. However in comparison, the extent of error in flow estimation is always less if a lower value of expansivity is considered rather than a value higher than the actual value. Comparison of the effects of error added for both Case I and Case II are shown in Table 9 (Appendix C).

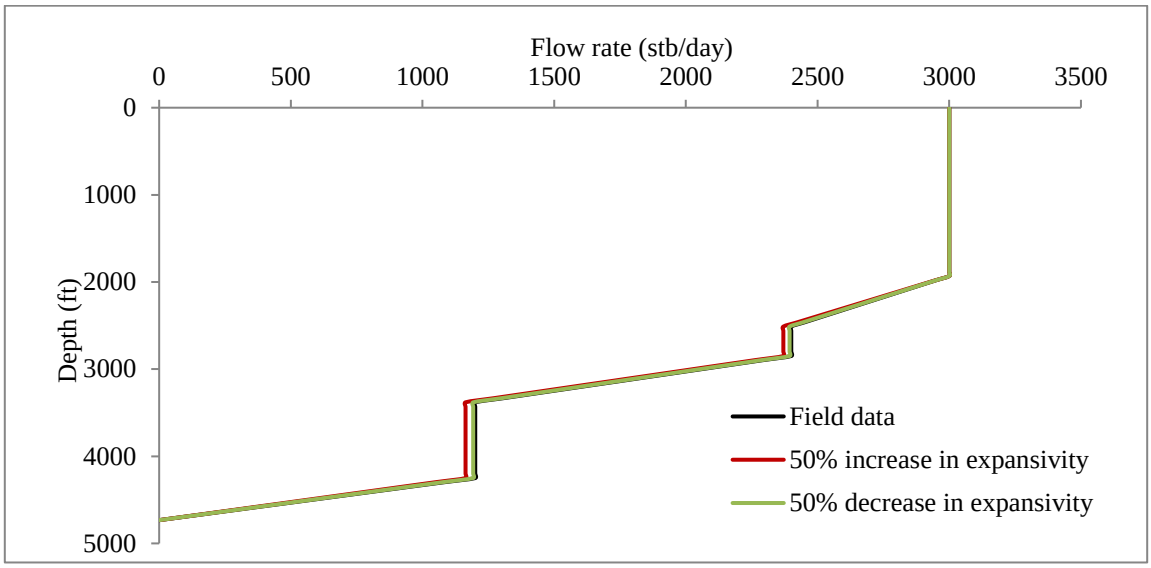

Fig. 20: A sensitivity analysis of flow profile to error in thermal expansivity for case II

Fig. 21 and Fig. 22 shows effect of well deviation on flow rate. Error in the angle of inclination of the well can have significant impact on flow rate estimation. Assuming an

inclination greater than the actual inclination gives a higher flow rate at a lower depth. For example, assuming no well inclination in case II where the well is actually 15 degrees inclined, gives us a 14 % higher flow rate at the bottomhole Table 10 (Appendix C). Therefore, knowledge of angle of deviation of well is very important for estimating a wellbore flow profile.

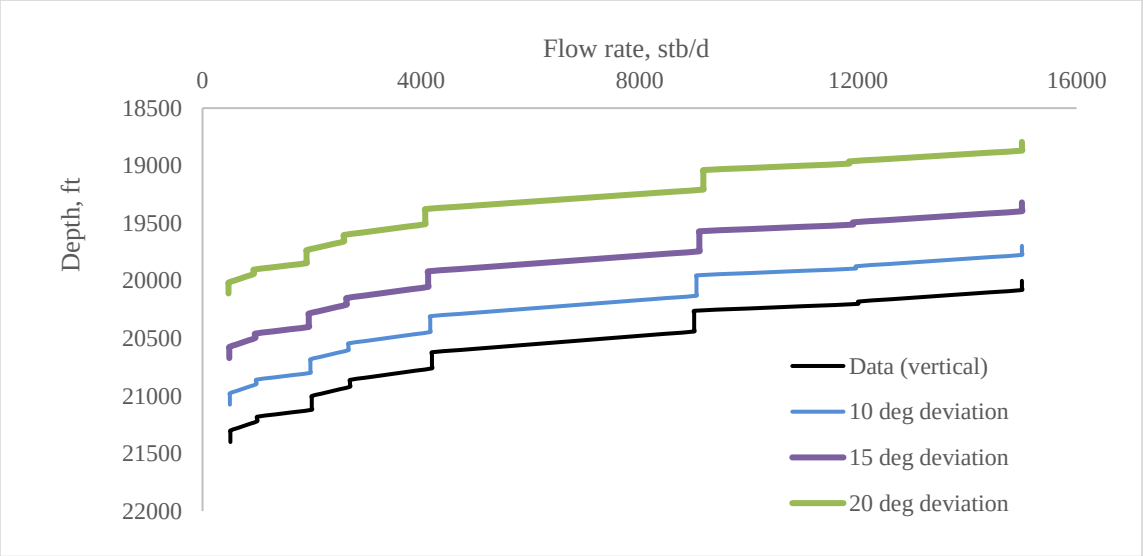

Fig. 21: A sensitivity analysis of flow profile to error in well inclination for case I

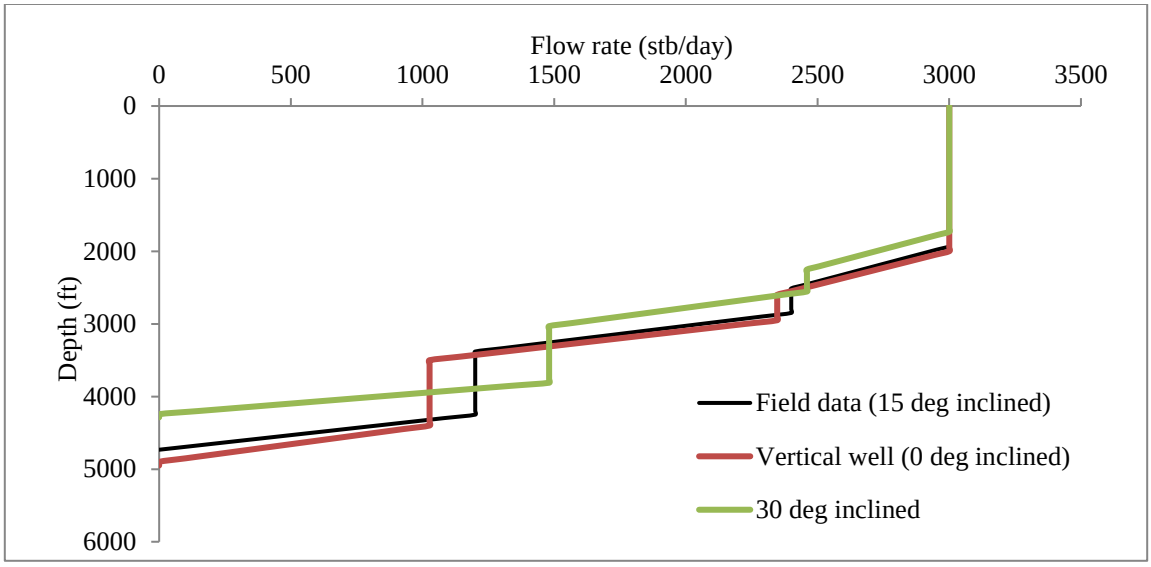

Fig. 22: A sensitivity analysis of flow profile to error in well inclination for case II

4.3 Design of Experiment

We performed Design of Experiment (DoE) with four variables namely: temperature, pressure, density of fluid and well deviation. The DoE illustrates the effects of these properties on the output, which in our case is flow profile. The procedure of performing the DoE is shown in detail in Appendix D.

DoE was performed on case I. The dependent variable is the flow rate at the bottom hole. To perform the DoE, error was added to each of the parameters under investigation. The errors added such that each parameter has an extreme but realistic high and low values. These are tabulated in Table 11 (Appendix D). The errors have been added to the whole data set along the wellbore, not only to the data at the bottom hole.

The main effects of the four variables are shown in Fig. 23. According to Fig. 23 flow profiling is most sensitive to temperature among the four variables. Followed by temperature, pressure has significant influence on flow rate calculation.

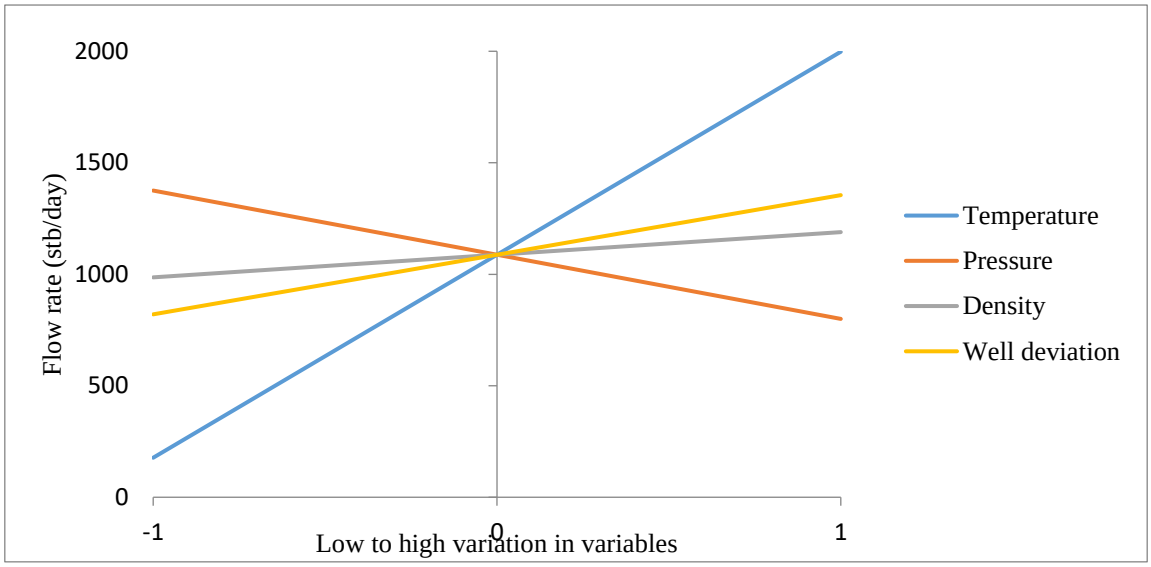

Fig. 23: Effects of main variables on bottom hole flow rate

Fig. 24 and Fig. 25 show the effects of interaction of two and more variables respectively on flow rate estimation.

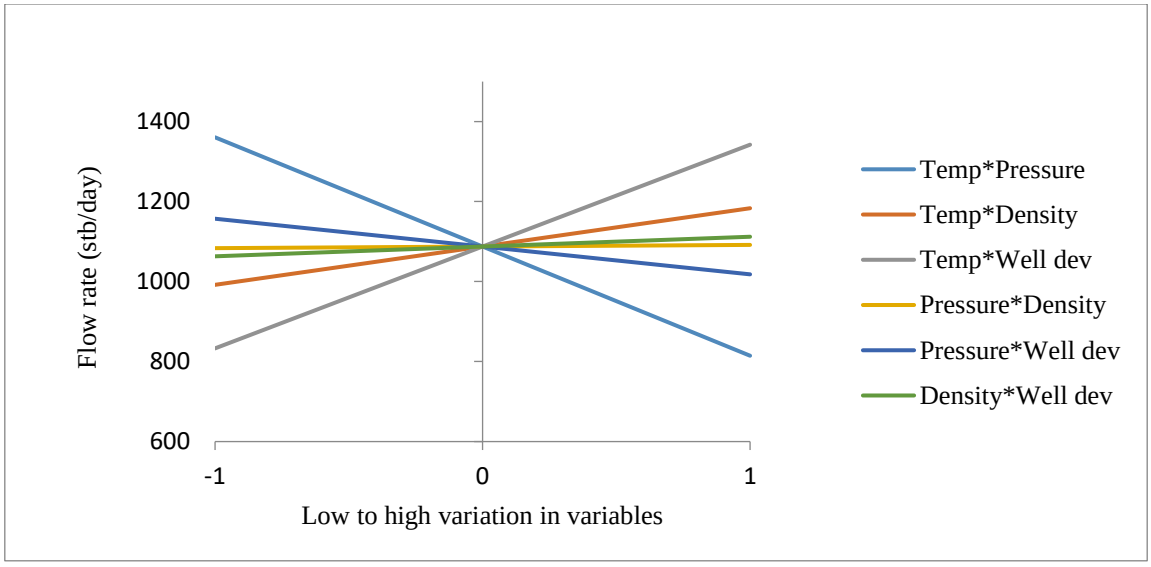

Fig. 24: Effects of interaction of two variables

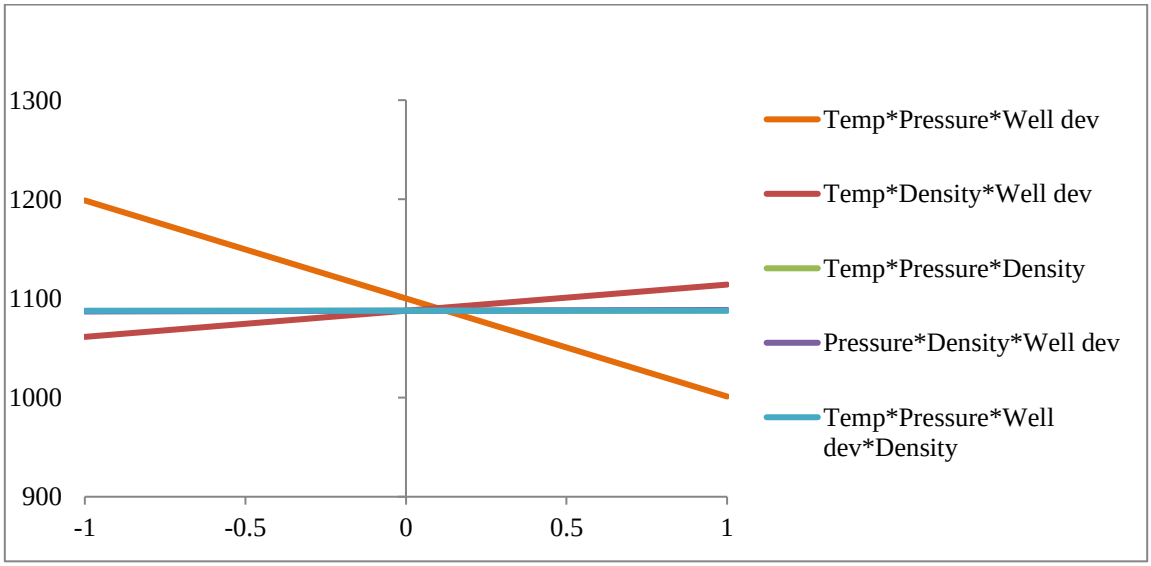

Fig. 25: Effects of interaction of more than two variables

In Fig. 25 three of the lines are almost overlapping (temperature*pressure*density, pressure*density*well deviation and temperature*pressure*density*well deviation). The other combinations of interaction (temperature*pressure*well deviation and temperature*density*well deviation) have greater slopes and leads to the conclusion that temperature, pressure and well deviation are the more sensitive properties.

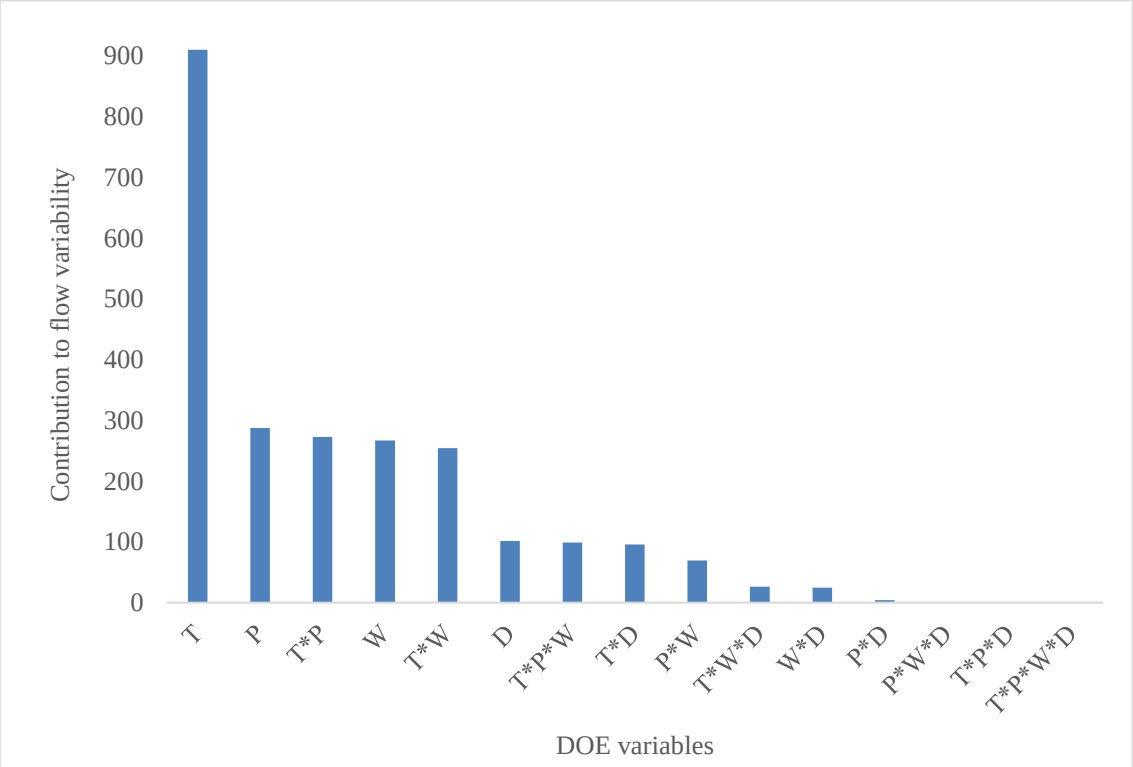

Fig. 26: Pareto chart showing effects for bottom hole flow rate

The pareto chart in Fig. 26 shows comparison of the effects of individual parameters as well as the effect of interaction of these parameters on bottomhole flow rate. In the pareto

chart *T* is temperature, *P* is pressure, *D* represents density and *W* represents well deviation. This sensitivity analysis leads us to the conclusion that temperature is the most critical parameter that influences the fluid flow. Next in line is fluid pressure followed by well deviation, however, their effects are much less significant compared to temperature of fluid. The impact of these parameters on bottomhole flow rate can also be displayed with more detail through a tornado chart as shown in Fig. 27. The tornado chart also shows the upper and lower limits of the parameters considered for performing the design of experiment and their impact on the range of flow rate variation.

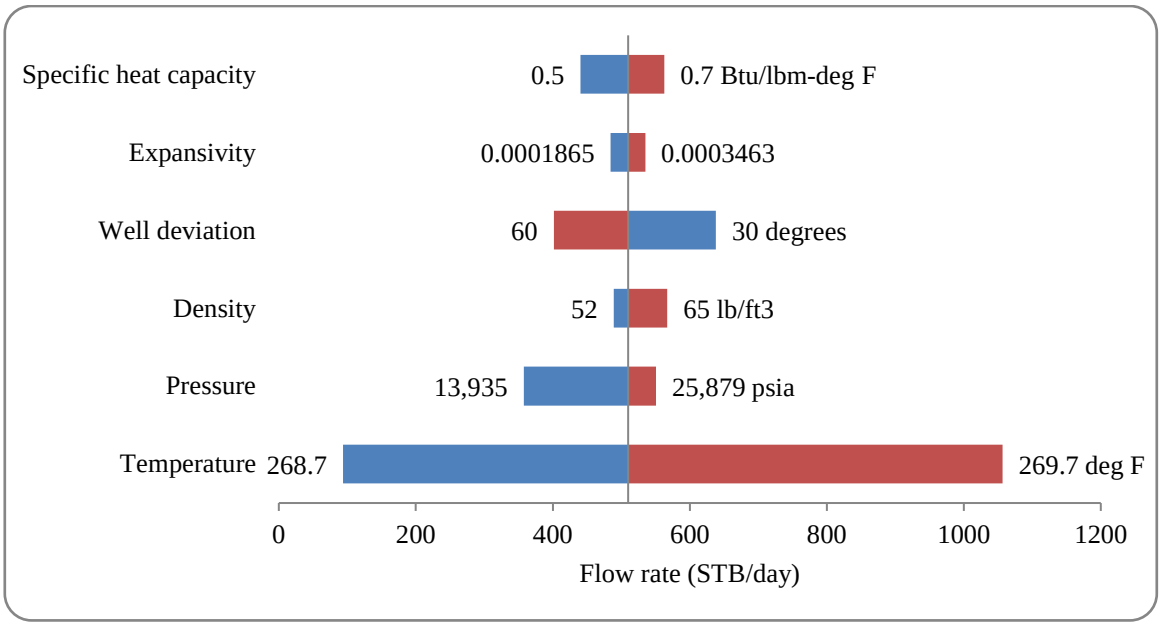

Fig. 27: Tornado chart illustrating impact of flow parameters on bottomhole flow rate

The study of sensitivity analysis and design of experiment described in this chapter helps us attain better idea about the impact of different parameters on flow rate estimation and

thereby on the flow profile. It also helps us understand which are the critical parameters for our model and the necessity of their accuracy as well as the extent of accuracy required. We only performed sensitivity analysis and design of experiment on one set of data but we would come to the same conclusion if applied on our field data. This is because we were able to crosscheck our method of data generation using the given field data.

CHAPTER V

CONCLUSIONS AND RECOMMENDATIONS

5.1 Conclusions

In this study, we developed a model that generates a flow profile for a well with multiple pay zone using pressure and temperature data. The model developed is applicable for two-phase flow as well as for single-phase oil flow. We applied energy and momentum balance in the wellbore system and its surrounding incorporating the pressure and temperature data to arrive at the final model. The model takes into account changes on fluid properties such as density and viscosity and the changes in fluid temperature due to Joule-Thompson effect. This model was then validated against available field data and proved to be satisfactorily accurate.

Sensitivity analysis of the various parameters showed that the accuracy of temperature is most critical to estimating the flow profile. Following temperature, pressure and well deviation are two important parameters that need to be reasonably accurate to obtain a fair estimate of flow rates. Other variables such as density, viscosity and specific heat capacities do not have much impact on the overall accuracy of the model, that is, the model can afford to have some error in these parameters. We also performed a design of experiment with four of the variables, which are temperature, pressure, well deviation, and density and came down to the same conclusion that temperature is the most critical parameter for this model.

In conclusion, the model we developed provides a reasonable estimate of flow rates at each section of a wellbore when there is production from multiple pay zones. The model is also applicable for two-phase flow and for deviated wells, which gives the model far more acceptability.

5.2 Recommendations for Future Work

The model we developed in this study can be used to give us a reasonable estimate of fluid flow profile along a wellbore. The model has been developed more importantly for applying in wells in deep water assets. However, the model may be modified to be applicable for use in other complex wellbore systems. Following are some recommendations for future work that may expand the applicability of the model.

1. Extend the study to single-phase gas flow.
2. Take into account changes in specific heat capacity throughout the well.
3. Expand the model to take into account the heat exchange between the formation and the wellbore fluid, Q.
4. Expand the model to apply to unconventional reservoirs by assuming linear flow production.
5. Apply the model to horizontal wells by incorporating appropriate flow models in the energy balance. While doing so also take into account the changes in fluid temperature in the wellbore due to Joule Thompson effect.
6. Expand the model to apply in semi-steady state operations.

REFERENCES

Bremer, K., E. Lewis, G. Leen et al. 2010. Fibre Optic Pressure and Temperature Sensor for Geothermal Wells. IEEE SENSORS 2010 Conference, 538-541.

Brown, G., D. Field, J. Davies et al. 2005. Production Monitoring Through Openhole Gravel-Pack Completions Using Permanently Installed Fiber-Optic Distributed Temperature Systems in the BP-Operated Azeri Field in Azerbaijan. 2005 SPE Annual Technical Conference and Exhibition, Dallas,TX, 1-6.

Champion, Brian Phillip. 2006. A Novel Wireless Solution To Address Uncertainties in Reservoir Connectivity. 2006 SPE Annual Technical Conference and Exhibition, San Antonio, Texas, 1-6.

Champion, Brian Phillip, E. A. Puntel. 2015. Reducing Reservoir Uncertainty During Appraisal and Development- Novel Applications of a new Wireless Reservoir Monitoring Technology in Santos Basin Pre-Salt. SPE Annual Technical Conference and Exhibition, Houston, Texas, 1-16.

Champion, Brian Phillip, Allison J. Strong, Neil Moodie. 2009. Mungo Platform: A New Wireless Retrofit Solution to Restore Real Time BHP/BHT Data After a Permanently Installed Monitoring System has Failed-A North Sea Case History. 2009 SPE Offshore Europe Oil & Gas Conference & Exhibition, Aberdeen, UK, 1-10.

Chevarunotai, N., A. R. Hasan, C. S. Kabir. 2015. Transient Flowing-Fluid Temperature Modeling in Oil Reservoirs for Flow Associated with Large Drawdowns. SPE Annual Technical Conference and Exhibition, Houston, Texas, 1-17.

Hasan, A. R., C. S. Kabir, X. Wang. 2009. A Robust Steady-State Model for Flowing-Fluid Temperature in Complex Wells. *SPEPO* (May 2009): 269-276.

Hasan, A.R., C.S. Kabir. 2002. *Fluid Flow and Heat Transfer in Wellbores*. Richardson, TX: SPE Textbook Series.

Hill, A.D. 1990. *Prouction Logging-Theoretical and Interpretive Elements*, Vol. 14, 28-29. Richardson, TX: SPE Monograph Series, Society of Petroleum Engineers.

Johnson, D., J. Sierra, J. Kaura et al. 2006. Successful Flow Profiling of Gas Wells Using Distributed Temperature Sensing Data. 2006 SPE Annual Technical Conference and Exhibition, San Antonio, Texas, 1-16.

Kabir, C.S., B. Izgec, A.R. Hasan et al. 2011. Computing flow profiles and total flow rate with temperature surveys in gas wells. *Journal of Natural Gas Science and Engineering*: 1-7.

Lenn, Chris, Fikri J. Kuchuk, Justin Rounce et al. 1998. Horizontal Well Performance Evaluation and Fluid Entry Mechanisms. 1998 SPE Annual Technical Conference and Exhibition New Orleans, Louisiana, 365-377.

Nath, D.K., D.B. Finley, J.D. Kaura et al. 2006. Real-Time Firber-Optic Distributed Temperature Sensing (DTS)-New Applications in the Oil Field. 2006 SPE Annual Technical Conference and Exhibition, San Antonio, Texas, 65-66.

Ouyang, Liang-Biao, Dave Belanger. 2004. Flow Profiling via Distributed Temperature Sensor (DTS) System-Expectation and Reality. SPE Annual Technical Conference and Exhibition, Houston, Texas, 1-14.

Poulisse, H., P. van Overschee, J.Briers et al. 2006. Continuous Well Production Flow Monitoring and Surveillance. 2006 SPE Intelligent Energy Conference and Exhibition, Amsterdam, Netherlands, 1-6.

Wang, Xiaowei, Terry R. Bussear, A. Rashid Hasan. 2010. Techniques to Improve Flow Profiling Using Distributed Temperature Sensing. SPE Latin American & Caribbean Petroleum Engineering Conference Lima, Peru, 1-10.

Webster, M., S. Richardson, C.Gabard-Cuoq et al. 2006. Well Surveillance With a Permanent Downhole Multiphase Flowmeter. *SPE Production & Operations* (August 2006): 388-393.

APPENDIX A

PROPERTY COMPUTATION

This appendix shows in detail all the different correlations used for determining properties of the flowing fluid. It also explains the use of these properties in calculating pressure of fluid along the wellbore.

The correlations used for property calculation and the step by step procedure followed are shown below.

1. Solution gas-oil ratio for unsaturated oil is estimated by Standing's correlation.

$$R_s = \gamma_g \left[\frac{P}{18} \times 10^{(0.125\gamma_o - 0.00091T)}\right]^{1.2048} \quad (A.1)$$

where $\gamma_g$is the specific gas gravity, $\gamma_o$is the specific oil gravity, P is the pressure in the wellbore and T is the temperature of fluid in the reservoir.

2. Oil viscosity for unsaturated oil is estimated with the correlations of Beggs and Robinson (1975) and Vasquez and Beggs (1980).

$$\mu_o = a\mu_{od}^b \quad (A.2)$$

where
$$a = 10.715(R_s + 100)^{-0.515} \quad (A.3)$$

$$b = 5.44(R_s + 150)^{-0.338} \quad (A.4)$$

$$\mu_{od} = 10^A - 1 \quad (A.5)$$

$$A = BT^{-1.163} \quad (A.6)$$

$$B = 10^C \quad (A.7)$$

$$C = 3.0324 - 0.02023\gamma_o \quad (A.8)$$

3. Oil formation volume factor for unsaturated oil is estimated by Standing's correlation.

$$B_o = 0.972 + 0.000147F^{1.1756} \quad (A.9)$$

where

$$F = R_s(\left(\frac{\gamma_g}{\gamma_o}\right)^{0.5} + 1.25T \tag{A.10}$$

4. Density of producing fluid in lb/ft^3,

$$\rho = \frac{\gamma_o \times 62.4 \times 5.615 + R_s \times \gamma_g \times 0.0764}{B_o \times 5.615} \tag{A.11}$$

5. In-situ fluid velocity in ft/s

$$v = \frac{4 \times 5.615 \times qB_o}{86400\ \pi d^2} \tag{A.12}$$

where q is the flow rate in STB/day and d is the internal diameter of tubing.

6. Reynolds number,

$$Re = \frac{\rho v d}{0.000672\ \mu_o} \tag{A.13}$$

7. Moody friction factor,

   For Re<4000,

$$f = \frac{64}{Re} \tag{A.14}$$

   For Re>4000, Moody friction factor is calculated from Chen equation,

$$f = \left[-4log\left\{\frac{\varepsilon}{3.7065} - \frac{5.0452}{Re} log\left(\frac{\varepsilon^{1.1098}}{2.8257} + \left(\frac{7.149}{Re}\right)^{0.8981}\right)\right\}\right]^{-2} \tag{A.15}$$

   where, relative pipe roughness,

$$\varepsilon = \frac{\epsilon}{d} \tag{A.16}$$

   and ϵ is the length of the protrusions on the pipe wall. For simplicity, we are not accounting for transition between laminar and turbulent flow.

8. Frictional pressure gradient,

$$\left(\frac{dp}{dz}\right)_f = \frac{f\rho v^2}{2g_c} \tag{A.17}$$

9. Pressure gradient due to hydrostatic head,

$$\left(\frac{dp}{dz}\right)_h = \frac{g}{g_c}\rho sin\alpha \qquad (A.18)$$

where α is the angle of inclination of the well.

10. Pressure gradient due to kinetic energy,

$$\left(\frac{dp}{dz}\right)_{KE} = \rho v \frac{dv}{dz} \qquad (A.19)$$

where *dv/dz* is the velocity gradient.

11. Total pressure drop,

$$\left(\frac{dp}{dz}\right)_{total} = \left(\frac{dp}{dz}\right)_f + \left(\frac{dp}{dz}\right)_h + \left(\frac{dp}{dz}\right)_h \qquad (A.20)$$

12. Pressure at a point Δz below the initial point,

$$P_{i+1} = P_i + \Delta z \left(\frac{dp}{dz}\right)_{total} \qquad (A.21)$$

APPENDIX B

PROPERTY DATA FOR SYNTHESIZED RESERVOIR CONDITION

In this study, we used synthesized fluid properties, well temperature and pressure data to develop the model and to test it before applying it on actual field data. We term this as our Case I for which the total surface production assumed is 15000 STB/d. Table 3 lists fluid properties and well dimensions for Case I.

Table 3: Wellbore dimensions and fluid properties for synthesized reservoir condition

Parameter	Value, unit
Internal tubing diameter	4.5 in
Reservoir outer radius	4000 ft
Pipe roughness	0.00015 ft
Geothermal gradient	0.01 ^{0}F/ft
Oil API gravity	29.039^{0}
Gas oil ratio	69 SCF/STB
Specific gas gravity	0.7
Specific heat capacity	0.6 Btu/lbm-^{0}F
Thermal expansivity	0.0002664 ^{0}R^{-1}
Surface tension	0.002816 Btu/lb.psi

The well is considered to be a 21,000 ft long vertical well perforated at seven different intervals based on pay zones. The inflow is uniform in each interval but is not the same for each interval. Table 4 lists the contributions of production in each interval.

Table 4: Fluid contribution from perforated intervals

Perforated intervals (ft)	Oil inflow (STB/d)
20080-20180	3000
20200-20260	3000
20440-20620	4800
20760-20860	1500
20920-21000	700
21120-21180	1000
21220-21300	490

APPENDIX C

EFFECTS OF ERROR ADDED TO PROPERTY DATA ON BOTTOMHOLE FLOW

For performing the sensitivity analysis errors were added to each of the six focused parameters: pressure, temperature, density, specific heat capacity, thermal expansivity and well deviation. Errors were added along the length of the wellbore. These added error resulted in error in the calculated bottomhole flow rate. The following tables show these effects for two different errors for each Case I and Case II.

Table 5: Effect in bottomhole flow calculation due to error added to pressure data

	Case I		Case II	
Error added in pressure data	10%	40%	10%	40%
Original bottomhole flowrate (stb/day)	510		200	
Oil flow rate calculated with error added to pressure (stb/day)	471.3	369.5	200.7	214.4
Error in total bottomhole flow rate	-8.2%	-38%	-0.34%	-7.18%

Table 6: Effect in bottomhole flow calculation due to error added to temperature data

	Case I		Case II	
Error added in temperature data	0.05^0C	1^0C	0.05^0C	1^0C
Original bottomhole flowrate (stb/day)	510		200	
Oil flow rate calculated with error added to temperature data (stb/day)	560	1645	197.5	218
Error in total bottomhole flow rate	9%	69%	1.27%	9%

Table 7: Effect in bottomhole flow calculation due to error added to density data

	Case I		Case II	
Error added in density	-10 lb/ft^3	+10 lb/ft^3	-10 lb/ft^3	+10 lb/ft^3
Original bottomhole flowrate (stb/day)	510		200	
Oil flow rate calculated with error added to density (stb/day)	433.2	567.1	206.3	189.6
Error in total bottomhole flow rate	-17.7%	10.1%	3.2%	5.1%

Table 8: Effect in bottomhole flow calculation due to error added to specific heat capacity

	Case I		Case II	
Error added in specific heat capacity ($Btu/lb_m\ ^0F$)	-0.1	+0.1	-0.1	+0.1
Original bottomhole flowrate (stb/day)	510		200	
Oil flow rate calculated with error added to specific heat capacity (stb/day)	435.3	567.9	204.7	190.4
Error in total bottomhole flow rate	-17%	+10%	2.4%	4.8%

Table 9: Effect in bottomhole flow calculation due to error added to thermal expansivity

	Case I		Case II	
Error added in thermal expansivity	-30%	+30%	-30%	+30%
Original bottomhole flowrate (stb/day)	510		200	
Oil flow rate calculated with error added to thermal expansivity (stb/day)	625.67	408.3	197.7	194.8
Error in total bottomhole flow rate	18.5%	-24.9%	1.1%	2.6%

Table 10: Effect in bottomhole flow calculation due to error added to well inclination

	Case I		Case II	
Error added in well inclination	5^0	15^0	5^0	15^0
Original bottomhole flowrate (stb/day)	510		200	
Oil flow rate calculated with error added to well inclination (stb/day)	507.3	490.0	183.0	171.1
Error in total bottomhole flow rate	-0.54%	-4.1%	8.5%	14.4%

APPENDIX D

DESIGN OF EXPERIMENT

Our model includes a number of factors that would influence the outcome the model. Through Design of Experiments, we can simultaneously determine the individual and interactive effects of multiple parameters of our study on the results.

We chose four parameters to see their individual and interactive effects on the bottomhole flow rate. These parameters are temperature, pressure, density and well deviation. For performing the DoE, errors were added to each parameter that have extreme but realistic high and low values. Since we chose four parameters we will have 16 (2^4) scenarios. We assign "+1" to represent the high value and "-1" to represent the low value. The input parameters are shown in Table 11.

Next, we ran the model 16 times to obtain the bottomhole flow rate for all combinations of +1's and -1's of the 4 elements. The results are shown in Table 12.

Table 11: Input parameters for design of experiment

Variables	-1 level	+1 level	Base	Error added
Temp	268.7	269.7	269.2	$\pm 0.5^0$C
Pressure	13935	25879	19948	± 30%
Density	52	65	55	Light oil to water density
Well deviation	30	60	0	Random

Table 12: Results of 16 different scenarios

Exp. No.	Temp	Pressure	Density	Well dev	Flow rate
1	-1	-1	-1	-1	181
2	+1	-1	-1	-1	1749
3	-1	+1	-1	-1	134
4	+1	+1	-1	-1	910
5	-1	-1	+1	-1	189
6	+1	-1	+1	-1	2035
7	-1	+1	+1	-1	155
8	+1	+1	+1	-1	1210
9	-1	-1	-1	+1	200
10	+1	-1	-1	+1	2982
11	-1	+1	-1	+1	172
12	+1	+1	-1	+1	1561
13	-1	-1	+1	+1	198
14	+1	-1	+1	+1	3468
15	-1	+1	+1	+1	189
16	+1	+1	+1	+1	2068

To observe the main effects on the bottomhole flow rate we calculated the average of each parameter for when it is "-1" and when it is "+1" and then calculate the total bottomhole flow variation due to that parameter. For example,

Average bottomhole flow for temperature "-1"

= (181+134+189+155+200+172+198+189)/8= 177

Average bottomhole flow for temperature "+1"

= (1749+910+2035+1210+2982+1561+3468+2068)/8 = 1998

Slope = (1998-177)/2 = 910

Similarly, the effects of individual variables and multiple variables in different combinations can be calculated (Table 13) and plotted for better estimation. These slopes are then plotted in a pareto chart. Pareto charts are a useful tool in Design of Experiments. Pareto charts make it easier to visualize and compare the effects of individual and combined effects of each variable.

Table 13: Contribution of DoE variables to flow variability

DoE variables	Contribution to flow variability
Temperature	910.3
Pressure	287.8
Temperature*Pressure	273.0
Well deviation	267.3
Temperature*Well deviation	254.6
Density	101.4
Temperature*Pressure*Well deviation	98.9
Temperature*Density	95.8
Pressure*Well deviation	69.5
Temperature*Well deviation*Density	26.4
Well deviation*Density	24.5
Pressure*Density	4.09
Pressure*Well deviation*Density	0.77
Temperature*Pressure*Density	0.21
Temperature*Pressure*Well deviation*Density	0.04